

**Annual Activity Report
on
Japan-ASEAN Science, Technology and
Innovation Platform (JASTIP),
Work Package 2 (WP2) –
Energy and Environment**

2017 Progress

TABLE OF CONTENTS

1. Innovations for Conversion of Biomass to High Value Chemicals by Photocatalytic Process	.4
1.1 Introduction and Rational	4
1.2 Project Scopes	6
1.3 Project Progress	6
1.4 Conclusions.....	14
1.5 Project Outputs.....	14
1.6 References	16
2. Development of Carbons from Biomass for Energy Storage Applications	20
2.1 Introduction	20
2.2 Literature Review	23
2.3 Experimental.....	34
2.4 Results and Discussion	36
2.5 Conclusions.....	44
2.6 Outputs	44
3. Innovations in Biomass Application for Catalytic Material Synthesis and Energy Devices	47
3.1 Purpose of Collaborative Research.....	47
3.2 Research Progress.....	47
3.3 Outputs	51

Innovations for Conversion of Biomass to High Value Chemicals by Photocatalytic Process

1. Innovations for Conversion of Biomass to High Value Chemicals by Photocatalytic Process

Surawut Chuangchote¹, Navadol Laosiripojana², Verawat Champreda³, Takashi Sagawa⁴

¹ Department of Tool and Materials Engineering, Faculty of Engineering, King Mongkut's University of Technology Thonburi (KMUTT), 126 Prachauthit Rd., Bangmod, Thungkru, Bangkok 10140, Thailand.

² The Joint Graduate School of Energy and Environment, Centre of Excellence on Energy Technology and Environment, King Mongkut's University of Technology Thonburi (KMUTT), 126 Prachauthit Rd., Bangmod, Thungkru, Bangkok 10140, Thailand.

³ National Center for Genetic Engineering and Biotechnology, 113 Phahonyothin Rd., Klong Luang, Pathumthani 12120, Thailand.

⁴ Graduate School of Energy Science, Kyoto University, Kyoto 606-8501, Japan.

Abstract

Application of photocatalytic processes for conversion of sugars which can be derived from lignocelluloses to energy and chemicals is considered a new promising environmentally friendly alternative which will play an important role in biorefinery and bioindustry related to valorization of sugars and agricultural wastes. This project aims to advance our technology on photocatalyst design based on the closed collaboration with Prof. Takashi Sagawa, Kyoto University under the JASTIP Renewable Energy program between NSTDA and Kyoto University (2015-2019). The project themes will cover (1) continual research on fabrication and modification of photocatalysts for conversion of sugars to high-value chemicals (e.g. functional sugar derivatives) by improving the catalyst's specificity by fabrication techniques or surface modification and (2) design and assembly of a prototype photocatalytic reactor. This concept on "photo-conversion on renewable biomaterials" will lead to the development of "photo-bio flow reactor" and will provide strong platform for conversion of sugars to value-added chemicals in integrative biorefinery.

Keyword Biomass, Photocatalysis, Sugar conversion, Lignin utilization, High-value chemicals, Sugar derivatives

1.1 Introduction and Rational

Thailand is an agricultural-based country where lignocellulosic biomass can be considered as an important renewable energy resource for production of electricity, heat, liquid fuel, and commodity chemicals. This "biorefinery" concept can alleviate global warming due to the carbon neutral nature of the biomass and decrease the country's dependence of the depleting fossil resource. Biomass is the renewable resources (sustainable), which has its compositions similar to fossil fuel (contains C and H), and the products obtained from biomass are similar to those of petroleum. In details, lignocellulosic biomass is a multi-structure material. It consists mainly of three polymers i.e. cellulose, hemicelluloses, and lignin, which are associated with each other in

addition to small amounts of acids, salts, and minerals. Currently several technologies, including catalytic, thermochemical, and biotechnological routes have been investigated for conversion of biopolymers-derived intermediates from various agricultural wastes to a spectrum of value-added products. However, these technologies are thermochemically and/or biochemically conversion processes which are limited by some restrictions in practice, such as high cost of reagents and equipment, high energy consumption, and harsh reaction conditions. Some processes have to use high chemical contents and more production steps for efficient biomass conversion into fuels and chemicals. These cause high capital investment in term of energy input and chemical usage. The exploration of new routes for the production of platform chemicals or fuels from biomass thus becomes increasingly important.

Photocatalysis is one of promising processes for energy and chemical productions, because it can be performed under solar irradiation at room temperature and mild condition. It offers the possibility of extending the spectrum of applications to a variety of processes, including oxidations and oxidative cleavages, reductions, isomerizations, substitutions, condensations, and polymerizations. In addition, it is considered as clean, effective, energy-saving, technology simple, ecologically benign, and low cost strategy. Photocatalysis is a well-established technique for many applications, e.g. wastewater or air treatment, pollutant degradation, and hydrogen (clean fuel) production by water splitting. Titanium dioxide (TiO_2) is the most important photocatalyst for many applications, such as degradation of organic pollutants (Hwang *et al.*, 2012), production of hydrogen (Gomathisankar *et al.*, 2013), self-cleaning surfaces (Murugan *et al.*, 2013), and dye sensitized solar cells (Cheng *et al.*, 2013). TiO_2 is a white solid inorganic substance that occurs naturally in several kinds of rock and mineral sands. It is a semiconducting material, which can be chemically activated by light with band-gap energy (E_g) of 3.2 eV. TiO_2 exists in 3 different crystalline modifications, i.e. anatase, brookite, and rutile, where anatase exhibits the highest overall photocatalytic activity (Park *et al.*, 2013). It is a popular catalyst to use in photocatalytic reactions, because TiO_2 has a highly oxidative, chemically stable, inexpensive, and nontoxic nature. TiO_2 nanoparticles have been prepared by different methods such as, chemical precipitation (Mashid *et al.*, 2006), chemical vapor deposition (CVD) (Shi, J., & Wang, X., 2011), sputtering (Song *et al.*, 2009), sol-gel technique (Bahadur *et al.*, 2011), hydrolysis, micro-emulsion method (Shen *et al.*, 2011), aerosol-assisted chemical vapor deposition (Tahir *et al.*, 2012), spray deposition (Bujnova *et al.*, 2010), thermal plasma (Tanaka *et al.*, 2011), hydrothermal method (Oh *et al.*, 2009), microwave-assisted hydrothermal synthesis (Melis *et al.*, 2012), solvothermal method (Zhang *et al.*, 2009), and the flame combustion method (Zhao *et al.*, 2007). Among these methods, sol-gel method is one of the most popular techniques for preparation of nanosized metal oxide materials with high photocatalytic activities (Su *et al.*, 2004; Tseng *et al.*, 2010).

In this proposed project, the application of photocatalytic approach for chemical production will be investigated based on the close collaboration between JGSEE, BIOTEC, and The University of Kyoto under the JASTIP Renewable Energy collaboration. The work will include the development of fabrication technology on synthesizing highly efficient photocatalysts and development of photocatalytic processes related to conversion of sugars and lignin to value-added chemicals. Together with the design and assembly of photocatalytic reactor with the concept on development of bio-energy devices in combination with efficient utilization of solar energy by Kyoto U., this collaboration will provide strong platform alternative technology for utilization of biomass in bio-industry which will contribute to the government's strategy on new S-curve industry.

1.2 Project Scopes

This project aims to develop high performance photocatalysts and photocatalytic reactor for production of target chemicals from glucose which can be obtained from 1st generation or 2nd generation raw materials in biorefinery. The project will focus on synthesis and fabrication of nano-scaled photocatalysts with improved performance and characterization of physicochemical properties of self-synthesized photocatalysts compared to commercial catalysts. The work will include the study of photocatalytic reactions on synthesis of high-value products (functional sugar derivatives) from glucose and application of the developed photocatalysts for production of target chemicals in photocatalytic reactor. The specific technical objectives are as follows:

- (a) To study the effects of fabrication conditions, doping and surface modification on morphological appearances, physico-chemical properties, photocatalytic activity and selectivity of the photocatalysts
- (b) To study the effects of chemical structures of sugars on mechanisms of photocatalytic reactions
- (c) To study the reaction pathways for photocatalytic conversion of sugars (e.g. glucose) to its derivatives or unconventional sugars
- (d) To design and assemble a prototype laboratory-scale photocatalytic reactor (photo bio-flow reactor)
- (f) To study the reaction kinetics on sugar conversion to target chemicals in photo-bio flow reactor

1.3 Project Progress

1.3.1 Photocatalytic conversion of glucose to high value fuels and chemicals

TiO₂ photocatalyst was synthesized by combination of sol gel and microwave with different concentrations of a surfactant, called CTAB. The surface morphology of the photocatalyst was observed using a scanning electron microscope. It was found that the agglomeration of TiO₂ photocatalyst decreased with increasing concentration of CTAB (**Fig. 1**). Therefore, the particle size of TiO₂ decreased with increasing concentration of CTAB. This is due to CTAB could reduce the surface tension and made high dispersion of TiO₂ precursor in the solution during the preparation process. In addition, CTAB could increase surface area of obtained catalysts, leading to high photocatalytic activity.

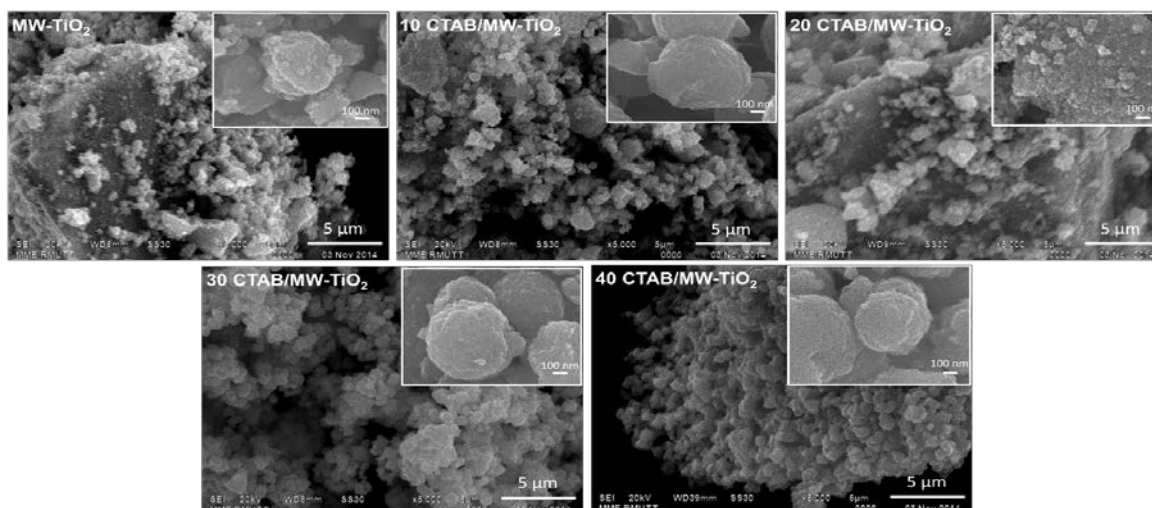


Fig. 1. SEM images of TiO₂ photocatalysts synthesized with different concentrations of CTAB.

The glucose conversions of various catalysts were carried out for 120 min under UV irradiation (wavelength = 365 nm). The results showed that high concentration of CTAB resulted in high glucose conversion. The highest glucose conversion of 60% represented in 40 CTAB/MW-TiO₂. It can conclude that high concentration of CTAB toward high surface area and low agglomeration of TiO₂, resulting in the highest glucose conversion (**Fig. 2**). The product yields of glucose conversion are shown in Fig. 3. There are 4 products of glucose conversion; gluconic acid, arabinose, xylitol, and formic acid. It was observed that the yields of all products tended to increase with increasing irradiation time. The highest conversion of 60% after 120 min showed the yield of gluconic acid, arabinose, xylitol, and formic acid of 5%, 26%, 3% and 25%, respectively. From the yields of products, it indicated that use of CTAB tended to give high yields of arabinose (**Fig. 3**).

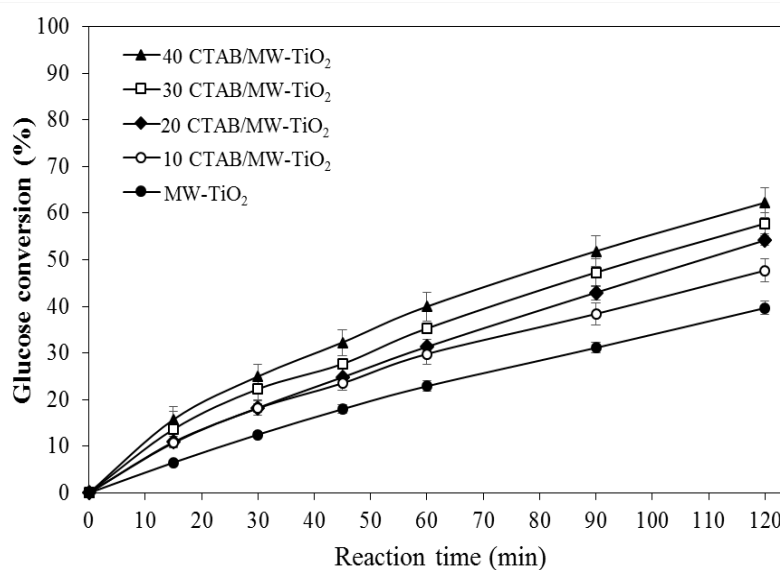


Fig. 2. Photocatalytic conversion of glucose with TiO₂ synthesized with different concentrations of CTAB in MW.

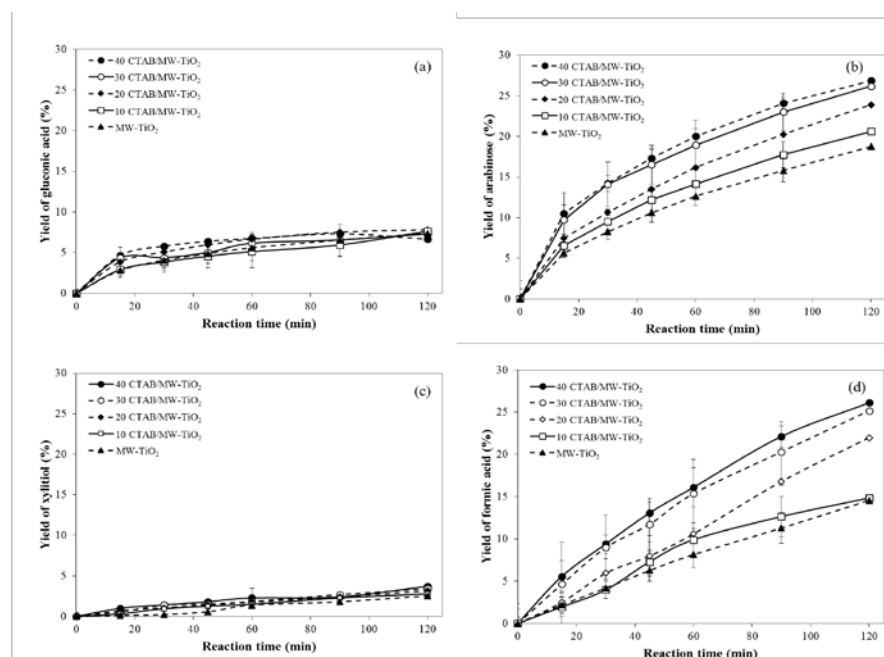


Fig. 3. Product yields of photocatalytic conversion of glucose with TiO₂ photocatalysts synthesized by different concentrations of CTAB.

As mentioned above, high surface area can enhance photocatalytic activity. So, the use of support materials is of interest for modification of TiO₂. The supports are expected to decrease agglomeration of TiO₂ and increase selectivity of photocatalytic reactions. From the group of supports, zeolites have been reported to delocalize band gap excited electrons of TiO₂ and thereby minimize electron-hole recombination to favor photoinduced electron-transfer reactions. SEM images show that surface morphology of zeolite changed after TiO₂ loading. It was found that the TiO₂ particles were coated on the surface (**Fig. 4**) compared with pristine zeolite. The TiO₂ coated on surface of zeolite showed well distribution. This caused the reduction of the agglomeration of TiO₂ nanoparticles synthesized with conventional process without zeolite. The catalyst size was increase when the amount of TiO₂ increased. Therefore, it was found that the specific surface area of TiO₂/ZeY increase compared with pure TiO₂.

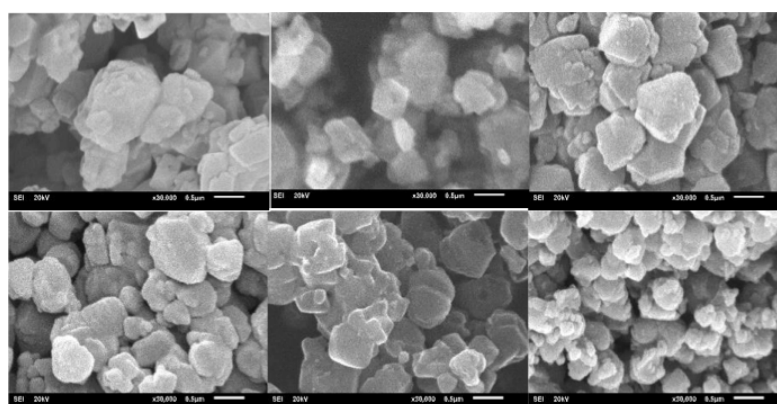


Fig. 4. SEM images (30000x) of ZeY, TiO₂(5%)/ZeY(95%), TiO₂(15%)/ZeY(85%), TiO₂(30%)/ZeY(70%), TiO₂(45%)/ZeY(55%), and TiO₂.

The glucose conversion and organic compound yields increased with long irradiation time and reached a maximum value at 120 min. The results showed that zeolite supported TiO_2 (TiO_2/ZeY) represented higher photocatalytic conversion of glucose than pristine TiO_2 (**Fig. 5**). However, it is distinct that the conversion rates did not increase linearly with increasing TiO_2 content. Certainly, the highest glucose conversion was achieved at a medium loading of 15% TiO_2 (75%) (Wang, C.C. *et al.* 2008). The yields of gluconic acid, arabinose, xylitol, and formic acid were 8.0, 29, 3, and 37%, respectively.

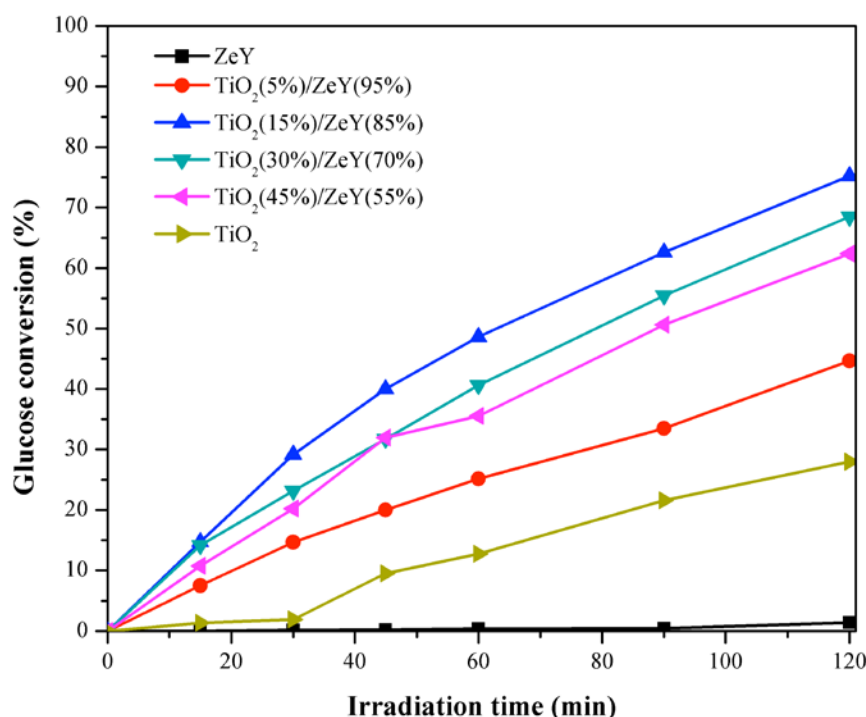


Fig. 5. Photocatalytic conversions of glucose under UV irradiation for 120 min with ZeY, TiO_2/ZeY (5, 15, 30, and 45 %wt), and TiO_2 .

1.3.2 Modification of photocatalyst by non-metal doping

The presence of non-metal (B, C, and N) could be enhance glucose conversion compared with bare- TiO_2 as shown in **Figure 6**. The single doping of nitrogen on TiO_2 was achieve glucose conversion with 60%. In addition, modified TiO_2 with co-doping of boron and nitrogen showed the highest glucose conversion up to 90% for 180 min. The yield of gluconic acid, arabinose, xylitol, and formic acid were 9.0, 30.5, 8.9 and 47.6%, respectively.

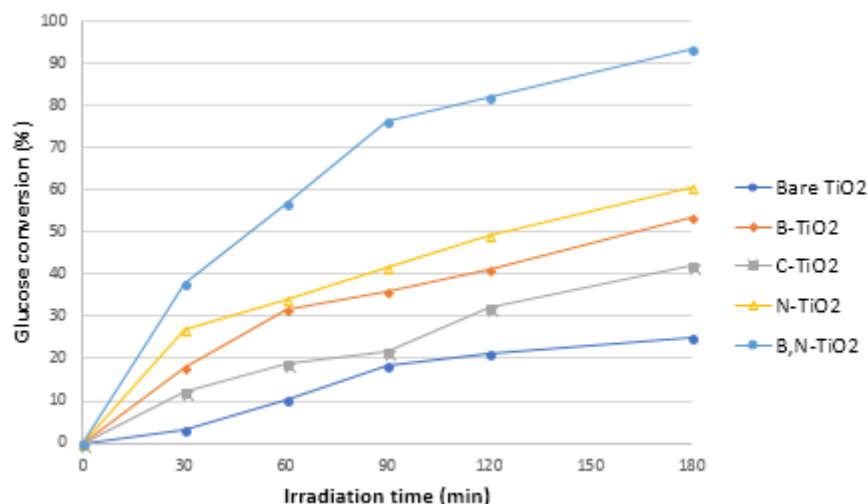


Fig. 6. Photocatalytic conversion of glucose under UV irradiation for 180 min in the presence of non-metal doping on TiO₂

The surface area of modified TiO₂ with non-metal is illustrated in **Table 1**. The increasing surface area was observed with the presence of C, B, N, and BN, respectively. This result was corresponded with the performance on glucose conversion. The presence of co-doping (BN) gave the highest surface area with 227.69 m²/g. Thus, high surface area leading to improve the active site on photocatalyst resulted in enhancement of photocatalytic activity as the same report in previous part.

Table 1. The specific surface area of non-metal doped on TiO₂

Samples	Pore size (nm)	Pore volume (cm ³ /g)	Surface area (m ² /g)
Bare TiO ₂	5.55	0.11	77.92
B-doped TiO ₂	3.99	0.15	147.37
C-doped TiO ₂	4.37	0.12	109.20
N-doped TiO ₂	5.47	0.21	153.04
BN-dopedTiO ₂	5.56	0.32	227.69

In addition, the increasing of productivity and conversion also supported with the results of PL measurement as shown in **Figure 7 and 8**. It was found that doping of non-metal on TiO₂ resulted in decreasing the intensity on PL measurement because of the effective inhibited the recombination of electron and hole. Moreover, UV-vis reflectance showed slightly shift of absorption in the visible region. A wide absorption region led to increase the excited electron under irradiation resulted in high performance on glucose conversion

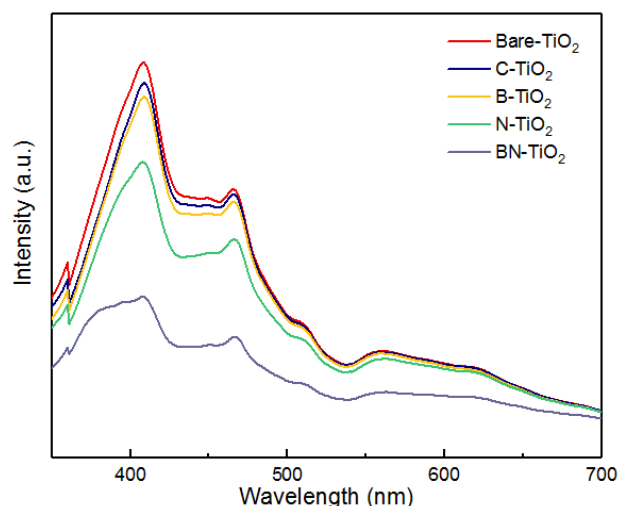


Fig. 7. Photoluminescence of non-metals doped TiO₂

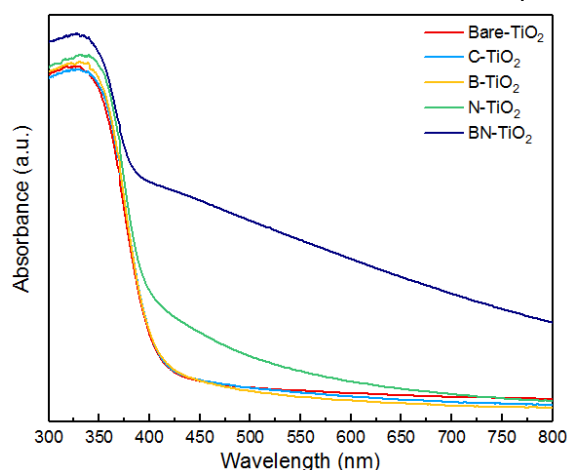


Fig. 8. UV-vis diffuse reflectance spectra of non-metal doped TiO₂

1.3.3 Photocatalytic conversion of glucose under visible light

In this study, the samples were irradiated under 450 W Xenon lamp equipped with sharp cut-off filter $\lambda > 380$ nm. The commercial of TiO₂ (P25) was used as benchmark as shown in **Figure 9**. The highest glucose conversion of P25 was observed at 9 h with 62%. The main product are formic acid and arabinose. Further, applied material as graphitic carbon nitride (g-C₃N₄) is a good candidate on photocatalytic conversion in term of productivity (**Figure 10**). The g-C₃N₄ could be enhance the conversion up to 77% at 12 h. Interestingly, the different main products of gluconic acid and formic acid were observed comparing with P25. The yield of gluconic acid, formic acid, arabinose, and xylitol were 35.2, 29.7, 8.9 and 4.4%, respectively.

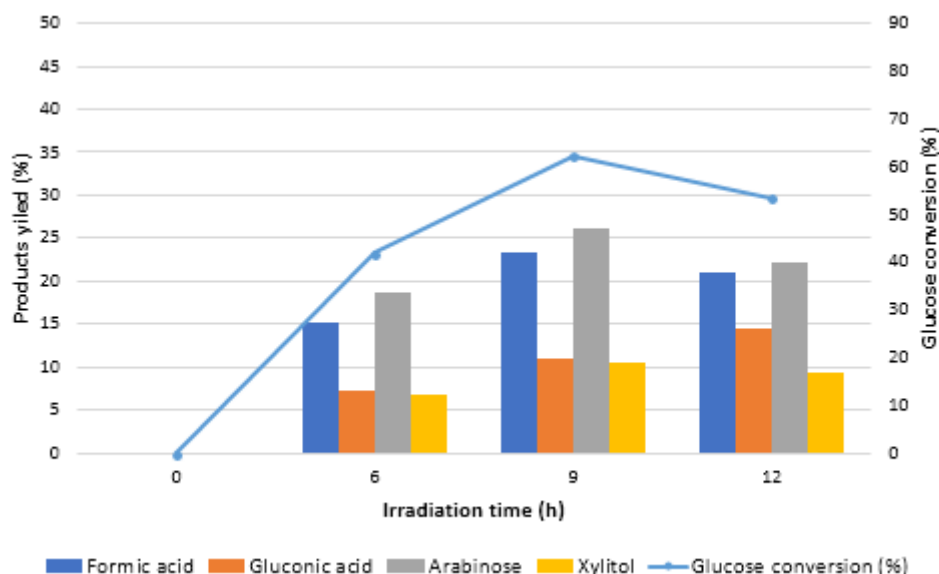


Fig.9. Photocatalytic conversion of glucose under visible light irradiation in the presence of TiO₂ (P25)

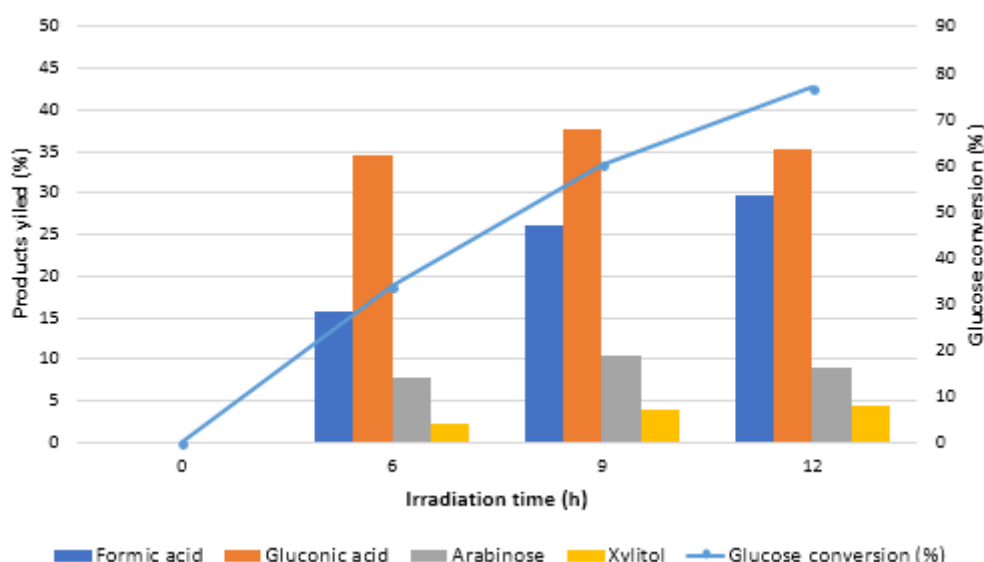


Fig.10. Photocatalytic conversion of glucose under visible light irradiation in the presence of graphitic carbon nitride (g-C₃N₄)

1.3.2 Photocatalytic conversion of lignin to high value fuels and chemicals

Cellulose is the main component of lignocellulosic, while lignin is the second abundant composition. So lignin has high potential for production of chemicals. There are many techniques to convert lignin to value added chemical, such as pyrolysis, gasification, and depolymerization. These technologies use high temperature and high energy consumption. So, photocatalytic is an interesting process. The photocatalytic conversion of kraft lignin catalyzed by P25 TiO₂ under UV irradiation present various products. The main products from lignin conversion are 2-methylnaphthalene, 4-hydroxy-benzaldehyde, and vanillin (**Fig. 11**).

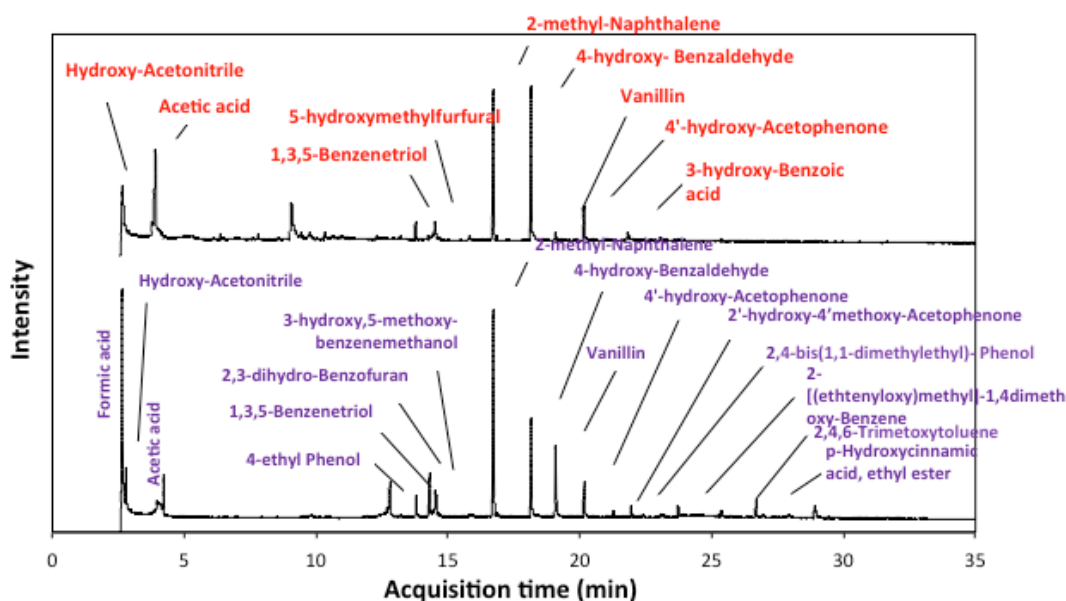


Fig.11. GC-MS spectra of hydrocarbon compounds derived from photocatalytic conversion of kraft lignin catalyzed by P25 TiO₂ under UV irradiation for 2 h and 5 h.

1.3.4 Combination of photocatalysis to conventional processes for enhancement of biomass pretreatment/hydrolysis

The pretreatment of biomass using photocatalytic process catalyzed P25 TiO₂ under UV irradiation for 24 h was preliminary carried out. The result showed that the amounts of individual sugar, as well as the total sugar yields, were low in the cases of no catalyst and no UV irradiation. TiO₂ photocatalysts could accelerate the separation of biomass compositions. Thus, a lot of products (native) were produced much compared with the photolysis (**Fig. 12**).

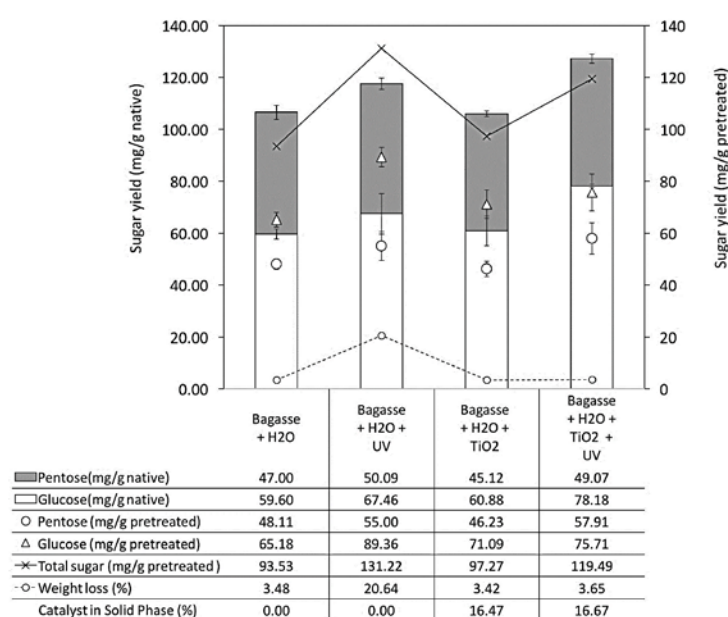


Fig. 12. Sugar digestibility yields in photocatalytic pretreatment (solvent = water) compared with blanks (no catalyst and/or no UV irradiation).

1.4 Conclusions

The photocatalytic reaction can convert glucose to value added chemical such as gluconic acid, arabinose, xylitol and formic acid. The modification of TiO₂ by CTAB and zeolite can improve the photocatalytic activity. TiO₂ can also be used as photocatalyst to convert lignin to value-added chemicals. Some high value chemicals, e.g. 2-methyl-naphthalene, 4-hydroxybenzaldehyde, and vanillin, were founded from the lignin conversion. Moreover, photocatalysis can be used for pretreatment of biomass. It was found that TiO₂ could accelerate the separation of biomass compositions better than photolysis.

1.5 Project Outputs

1.5.1 Publications (The publications in blue do not acknowledge JST as I mentioned to you before. Papers from number 7 has already cited JST.)

1. Navaporn Kaerkittha, Surawut Chuangchote, and Takashi Sagawa (2016) "Control of physical properties of carbon nanofibers obtained from coaxial electrospinning of PMMA and PAN with adjustable inner/outer nozzle-ends," *Nanoscale Research Letters*, 11(1), 1-9.
2. Witchaya Arpavate, Surawut Chuangchote, Navadol Laosiripojana, Jatuphorn Wootthikanokkhan, and Takashi Sagawa (2016) "ZnO Nanorod Arrays Fabricated by Hydrothermal Method Using Different Thicknesses of Seed Layers for Applications in Hybrid Photovoltaic Cells," *Sensors and Materials*, 28(5), 403-408.
3. Kamonchanok Roongraun, Navadol Laosiripojana, Surawut Chuangchote (2016) "Development of Photocatalytic Conversion of Glucose to Value-added Chemicals by Supported-TiO₂ Photocatalysts," *Applied Mechanics and Materials*, 839, 39-43.
4. Mathana Wongaree, Siriluk Chiarakorn, Surawut Chuangchote, and Takashi Sagawa (2016) "Photocatalytic Performance of Electrospun CNT/TiO₂ Nanofibers in a Simulated Air Purifier under Visible Light Irradiation," *Environmental Science and Pollution Research*, 23, 21395-21406.
5. Navaporn Kaerkittha, Surawut Chuangchote, Kan Hachiya, and Takashi Sagawa (2017) "Influence of the Viscosity Ratio of Polyacrylonitrile/Poly(methyl methacrylate) Solutions on Core-Shell Fibers Prepared by Coaxial Electrospinning", *Polymer Journal*, 49, 497-502.
6. Jiraporn Payormhorm, Surawut Chuangchote, Kunlanan Kiatkittipong, Siriluk Chiarakorn, and Navadol Laosiripojana (2017) "Xylitol and Gluconic Acid Productions via Photocatalytic-Glucose Conversion Using TiO₂ Fabricated by Surfactant-Assisted Techniques: Effects of Structural and Textural Properties", *Materials Chemistry and Physics*, 196, 29-36.
7. Jiraporn Payormhorm, Surawut Chuangchote, and Navadol Laosiripojana (2017) "CTAB-Assisted Sol-microwave Method for Fast Synthesis of Mesoporous TiO₂ Photocatalysts for Photocatalytic Conversion of Glucose to Value-added Sugars", *Materials Research Bulletin*, 95, 546-555.
8. Nutsanun Klueb-arb, Surawut Chuangchote, Kamonchanok Roongraung, Navadol Laosiripojana, and Takashi Sagawa (2017) "Fabrication of Several Metal-Doped TiO₂ Nanoparticles and Their Physical Properties for Photocatalysis in Energy and Environmental Applications", *Journal of Sustainable Energy & Environment*, accepted.

9. Puangphen Hongdilokkul, Surawut Chuangchote, Navadol Laosiripojana, and Takashi Sagawa (2017) "Conversion of Lignin via Photocatalysis Using Synthesized Ag-TiO₂ Photocatalysts Sintered under Different Atmospheres", Journal of Sustainable Energy & Environment, accepted.

1.5.2 Conference Proceeding

1. Navaporn Kaerkitcha, Surawut Chuangchote, Takashi Sagawa, Control of the physical properties of carbon nanofibers obtained from coaxial electrospinning of PAN and PMMA with adjustable inner/outer nozzle ends, EMN Hong Kong Meeting, Hong Kong, PRC, 2016/12/10.
2. Navaporn Kaerkitcha, Surawut Chuangchote, Takashi Sagawa, Control of the physical properties of carbon nanofibers obtained from coaxial electrospinning of PAN and PMMA with adjustable inner/outer nozzle ends, Ajou – Kyoto University Joint Symposium 2016, Swon, South Korea, 2016/1/28.
3. Navaporn Kaerkitcha, Surawut Chuangchote, Kan Hachiya, Takashi Sagawa, "Suitable outer/inner viscosity ratio of polymer solutions for fabrication of core-shell fibers by coaxial electrospinning," The 11th SPSJ International Polymer Conference (IPC2016), Fukuoka, 2016/12/16.
4. Kamonchanok Roongraun, Navadol Laosiripojana, and Surawut Chuangchote, 2015, "Development of Photocatalytic Conversion of Glucose to Value-added Chemicals by Supported-TiO₂ Photocatalysts," World Future Alternatives (Naresuan University, Phitsanulok, November 30-December 2), School of Renewable Energy Technology.
5. Jiraporn Payormhorm, Xiaobo Li, Thomas Maschmeyer, Navadol Laosiripojana, and Surawut Chuangchote, 2016 "The Study of Photocatalytic Oxidation of Benzyl Alcohol with g-C₃N₄ under Visible Light: Effect of pH and Salt," 2016 5th International Conference on Material Science and Engineering Technology (ICMSET 2016) (Tokyo, Japan, October 29-31), University of Tokyo.
6. Patcha Pattanapibul, Surawut Chuangchote, Navadol Laosiripojana, Verawat Champreda, Jerawut Kaewsaneee, 2017 "Enhancement of Enzymatic Hydrolysis and Lignin Removal of Bagasse Using Photocatalytic Pretreatment," The 3rd International Conference on Renewable Energy Technologies (ICRET2017) (Thammasat University, Bangkok, Thailand, January 22-24), ICRET Organization.
7. Surawut Chuangchote, 2017 "Electrospun TiO₂ Nanofibers Composed of Bundle of Aligned Nanofibrils: Fabrication, Structural and Photoluminescent Properties," 11th South East Asian Technical University Consortium (Ho Chi Minh City University of Technology (HCMUT), Vietnam, March 13-15), Ho Chi Minh City University of Technology.
8. Puangphen Hongdilokkul, Surawut Chuangchote, Navadol Laosiripojana, Takashi Sagawa, 2017 "Effects of Sintering Conditions in Ag-TiO₂ Nanoparticles on Photocatalytic Degradation of Lignin," International Conference on Materials Processing Technology 2017 (MAPT 2017) (Ramada Plaza Bangkok Menam Riverside, Bangkok, November 30-December 1), King Mongkut's University of Technology Thonburi, NM_01.
9. Nutsanun Klueb-arb, Surawut Chuangchote, Navadol Laosiripojana, Takashi Sagawa 2017 "Modifications of TiO₂ Nanoparticle Catalysts by Dopes with Transition Metals (Ag and Cu) or Alkali Metal (Rb)," International Conference on Materials Processing Technology 2017 (MAPT 2017) (Ramada Plaza Bangkok Menam Riverside, Bangkok, November 30-December 1), King Mongkut's University of Technology Thonburi, NM_01.

1.5.3 Award

1. The Best Presentation Award in The 3rd International Conference on Renewable Energy Technologies (ICRET2017) (Ms. Patcha Pattanapibul).

1.5.4 Exchange Researches

Table 1. Exchange researches in JASTIP

Name	Exchange Period	Research Topic
Ms. Kamonchanok Roongraung	18 Feb 2016 - 19 July 2016	Nano-scaled Photocatalysts for Energy Applications
Mr. Suriyachai Nopparat	28 Sep 2016 - 31 May 2017	Modification of Visible Light Photocatalytic Activity for Biomass Conversion to Value-added Chemicals
Ms. Nutsanun Klueb-arb	14 Nov 2016 - 23 Dec 2016	A Study of Reaction Pathways in Photocatalytic Conversion of Sugars to High-Value Fuels and Chemicals
Ms. Puangphen Hongdilokkul	14 Nov 2016 - 23 Dec 2016	Photocatalytic Upgrading of Lignin to High Value Products by Nanostructured Catalysts
Ms. Kanyanee Sanglee	6 Feb 2017 - 17 Mar 2017	Development of Visible-Light Irradiation Responded Metal Oxide for Photocatalytic and Photovoltaic Applications
Ms. Nattida Srisasiwimon	29 May 2017 - 29 June 2017	Modification of Photocatalysts for Lignin Conversion
Ms. Oranoot Sittipunsakda	29 May 2017 - 29 June 2017	Development of Metal-doped Photocatalysts for Hydrogen Evolution

1.6 References

Awungacha, L. C., Hild, J., Czermak, P., and Herrenbauer, M. (2014). Photocatalytic active coatings for lignin degradation in a continuous packed bed reactor, *International Journal of Photoenergy*, 2014.

Bahadur, N., Jain, K., Pasricha, R., and Chand, S. (2011), Selective gas sensing response from different loading of Ag in sol-gel mesoporous titania powders, *Sensors and Actuators B: Chemical*, **159**, 1, pp. 112-120.

Chaudhary, V., Srivastava, A.K., and Kumar, J. (2011), On the Sol-gel Synthesis and Characterization of Titanium Oxide Nanoparticles, *Materials Research Society*, **1352**.

Cheng, G., Akhtar, M.S., Yang, O.B., and Stadler, F.J. (2013), Structure modification of anatase TiO₂ nanomaterials-based photoanodes for efficient dye-sensitized solar cells, *Electrochimica acta*, **113**, pp. 527-535.

- Colmenares J.C., Magdziarz A., and Bielejewska A. (2011), High-value chemicals obtained from selective photo-oxidation of glucose in the presence of nanostructured titanium photocatalysts, *Bioresource Technology*, **102**, pp. 11254-11257.
- Fan, H. X., Li, H. P., Liu, Z. H., Yang, F., and Li, G. (2015). Production of fine chemicals by integrated photocatalytic degradation of alkali lignin solution in corrugated plate reactor and cyclic extraction technology, *Industrial Crops and Products*, **74**, 497-504.
- Gomathisankar, P., Yamamoto, D., Katsumata, H., Suzuki, T., and Kaneco, S. (2013), Photocatalytic hydrogen production with aid of simultaneous metal deposition using titanium dioxide from aqueous glucose solution, *International Journal of Hydrogen Energy*, **38**, pp. 5517-5524.
- Hwang, K.J., Lee, J.W., Shim, W.G., Jang, H.D., Lee, S.I., and Yoo, S.J. (2012), Adsorption and photocatalysis of nanocrystalline TiO₂ particles prepared by sol-gel method for methylene blue degradation, *Advance Powder Technology*, **23**, pp. 414-418.
- Jaimy, K. B., Vidya, K., Saraswathy, H. U. N., Hebalkar, N. Y., and Warriar, K. G. K. (2014), Dopant-free anatase titanium dioxide as visible-light catalyst: Facile sol-gel microwave approach, *Journal of Environmental Chemical Engineering*.
- Li, H., Lei, Z., Liu, C., Zhang, Z., and Lu, B. (2015). Photocatalytic degradation of lignin on synthesized Ag–AgCl/ZnO nanorods under solar light and preliminary trials for methane fermentation, *Bioresource Technology*, **175**, 494-501.
- Moza S., Heciak A., and Morawski A.W. (2011), Photocatalytic acetic acid decomposition leading to the production of hydrocarbons and hydrogen on Fe-modified TiO₂, *Catalysis Today*, **161**, pp. 189-195.
- Murugan, K., Subasri, R., Rao, T.N., Gandhi, A.S., and Murty, B.S. (2013), Synthesis, characterization and demonstration of self-cleaning TiO₂ coatings on glass and glazed ceramic tiles, *Progress in Organic Coatings*, **76**, pp. 1756-1760.
- Mutuma, B. K., Shao, G. N., Kim, W. D., and Kim, H. T. (2015), Sol-gel synthesis of mesoporous anatase-brookite and anatase-brookite-rutile TiO₂ nanoparticles and their photocatalytic properties, *Journal of colloid and interface science*, **442**, pp. 1-7.
- Nasralla, N., Yeganeh, M., Astuti, Y., Piticharoenphuna, S., Shahtahmasebi, N., Kompany, A., Karimipour, M., Mendis, B.G., Poolton, N.R.J., Siller, L., 2013, "Structural and spectroscopic study of Fe-doped TiO₂ nanoparticles prepared by sol–gel method", *Scientia Iranica*, Vol. 20, pp. 1018-1022.
- Oh, J. K., Lee, J. K., Kim, S. J., and Park, K. W. (2009), Synthesis of phase- and shape-controlled TiO₂ nanoparticles via hydrothermal process, *Journal of Industrial and Engineering Chemistry*, **15**, 2, pp. 270-274.
- Prado, R., Erdocia, X., and Labidi, J. (2013). Effect of the photocatalytic activity of TiO₂ on lignin depolymerization, *Chemosphere*, **91**(9), 1355-1361.
- Park, J.Y., Yun, J.J., Hwang, C.H., and Lee, I.H. (2010), Influence of silver doping on the phase transformation and crystallite growth of electrospun TiO₂ nanofibers, *Materials Letters*, **64**, pp. 2692-2695.

- Shen, X., Zhang, J., and Tian, B. (2011), Microemulsion-mediated solvothermal synthesis and photocatalytic properties of crystalline titania with controllable phases of anatase and rutile, *Journal of hazardous materials*, **192**, 2, pp. 651-657.
- Shi, J., & Wang, X. (2011). Growth of rutile titanium dioxide nanowires by pulsed chemical vapor deposition. *Crystal Growth & Design*, **11**(4), 949-954.
- Shojaie, A.F., and Loghmani, M.H. (2010), La³⁺ and Zr⁴⁺ co-doped anatase nano TiO₂ by sol-microwave, *Chemical Engineering Journal*, **157**, pp. 263-269.
- Song, S., Yang, T., Li, Y., Pang, Z., Lin, L., Lv, M., and Han, S. (2009), Structural, electrical and optical properties of ITO films with a thin TiO₂ seed layer prepared by RF magnetron sputtering, *Vacuum*, **83**, 8, pp. 1091-1094.
- Su, C., Hong, B.Y., and Tseng, C.M. (2004), Sol-gel preparation and photocatalysis of titanium dioxide, *Catalysis today*, **96**, pp. 119-126.
- Suwarnkar, M. B., Dhabbe, R. S., Kadam, A. N., & Garadkar, K. M. (2014). Enhanced photocatalytic activity of Ag doped TiO₂ nanoparticles synthesized by a microwave assisted method. *Ceramics International*, **40**(4), 5489-5496.
- Tahir, A.A., Peiris, T.A., and Wijayantha, K.G. (2012), Enhancement of Photoelectrochemical Performance of AACVD-produced TiO₂ Electrodes by Microwave Irradiation while Preserving the Nanostructure, *Chemical Vapor Deposition*, **18**, 4-6, pp. 107-111.
- Tanaka, Y., Sakai, H., Tsuke, T., Uesugi, Y., Sakai, Y., and Nakamura, K. (2011), Influence of coil current modulation on TiO₂ nanoparticle synthesis using pulse-modulated induction thermal plasmas, *Thin Solid Films*, **519**, 20, pp. 7100-7105.
- Tobaldi, D. M., Škapin, A. S., Pullar, R. C., Seabra, M. P., & Labrincha, J. A. (2013). Titanium dioxide modified with transition metals and rare earth elements: phase composition, optical properties, and photocatalytic activity. *Ceramics International*, **39**(3), 2619-2629.
- Vijayalakshmi, R., and Rajendran, V. (2012), Synthesis and characterization of nano-TiO₂ via different methods, *Arch App Sci Res*, **4**, 2, pp. 1183-1190.
- Zhang, Y., Zheng, H., Liu, G., and Battaglia, V. (2009), Synthesis and electrochemical studies of a layered spheric TiO₂ through low temperature solvothermal method, *Electrochimica Acta*, **54**, 16, pp. 4079-4083.
- Zhao, Y., Li, C., Liu, X., Gu, F., Jiang, H., Shao, W., and He, Y. (2007), Synthesis and optical properties of TiO₂ nanoparticles, *Materials Letters*, **61**, 1, pp. 79-83.

Development of Carbons from Biomass for Energy Storage Applications

2. Development of Carbons from Biomass for Energy Storage Applications

List of project participants

Thai side	Japan Side
MTEC/NSTDA - Dr. Sumittra Charojrochkul - Dr. Yatika Somrang - Mr. Thanathon Sesuk	Kyoto University - Prof. Dr. Takeshi Abe - Dr. Yuto Miyahara
Silpakorn University - Dr. Worapon Kiatkittipong - Ms. Chulita Pornpitakdamrong	

2.1 Introduction

2.1.1 Background and rationale

Thailand is an agricultural-based country which produces large amount of biomass but the majority of this abundant resources, especially agricultural leftover, has not yet been exploited extensively. Currently, the use of biomass in fuel application has been widely studied and practiced in order to reduce the reliance on petroleum-derived fuels. Not only its benefit as a substitute to conventional fuels, but bio-based economy can also be developed based on biomass. Biomass which mainly contains cellulose, hemicellulose and lignin can be converted into chemicals or valuable products. In fact, biomass is a major carbon source which can potentially be used in energy storage devices. Recently, there have been many previous works investigating the potential of using biomass as a source to produce carbons from carbonisation/hydrothermal carbonisation and/or chemical activation for energy storage application. However, none of the work has attempted to comprehend the effect of biomass constituents on the electrochemical characteristics for energy storage devices. In addition, the production of high-quality carbon materials from ‘challenging’ biomass, i.e. ash-containing biomass, particularly palm empty fruit bunch (PEFB), has not yet well established. This project, hence, aims to understand the role of precursor constituents on the electrochemical properties of the carbons and to develop method/conditions for the activated carbon production from palm empty fruit bunch using carbonisation/hydrothermal and/or chemical activation. This work is jointly collaborated between MTEC/NSTDA, responsible for producing carbon from biomass and performing physical characterisation of the obtained carbon, and Kyoto University, in charge of conducting electrochemical characterisation of the carbons for lithium-ion battery and supercapacitor applications.

2.1.2 Objectives

The objectives of this work are:

- To obtain more understanding of how each biomass constituent plays a part in the properties of activated carbons
- To gain more understanding on the influence of different carbonisation conditions and porogens on the properties of activated carbons
- To establish optimal carbonisation conditions for the production of activated carbons
- To explore the usage possibility of PEFB in Thailand as raw materials for energy storage devices

2.1.3 Expected outputs

- Knowledge on how each biomass constituent contributes to the properties of activated carbons
- Knowledge on how the carbonisation conditions and porogens affect the properties of activated carbon
- Optimal carbonisation conditions for the production of activated carbons as components for energy storage devices
- Usage viability of PEFB as raw materials for energy storage devices

2.1.4 Scope of study

The schematics of overall research scope and plan is shown in Figure 1-1. These objectives are planned to achieve in 5 years as tabulated in Table 1-1. The first part of the overall research scheme accounts for 2 years, i.e. 2017 and 2018.

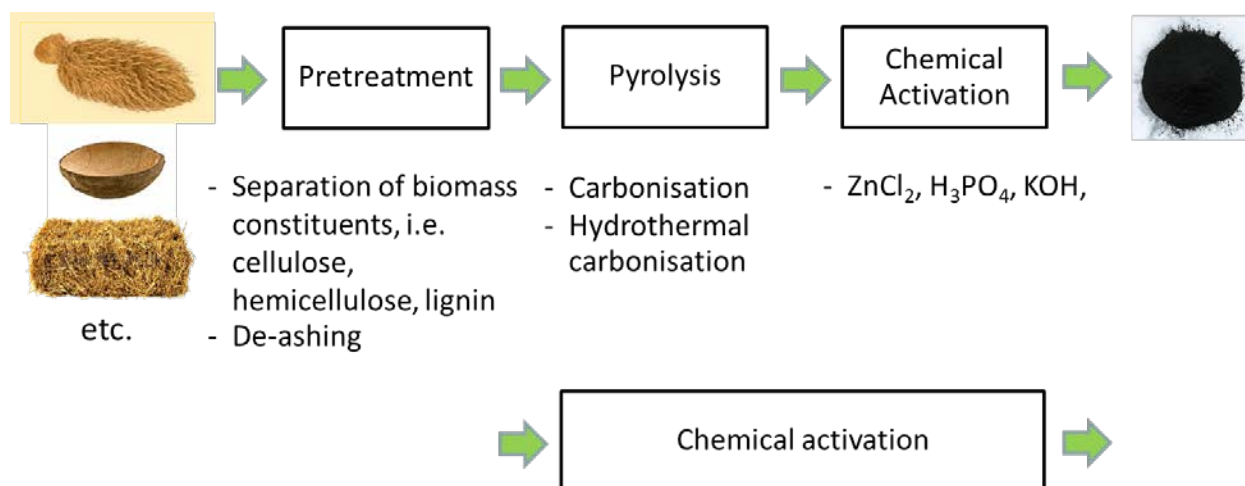


Figure 1-1 Schematics of overall research plan

Table 1-1 Research plan

Year	Plan
2017-2018	- Carbonisation of Thai agricultural residues
	- Carbonisation of pretreated PEFB*
	- Chemical activation of chars from carbonisation
	- Chemical activation of pretreated PEFB chars
2019-2020	- Hydrothermal carbonisation of Thai agricultural residues
	- Hydrothermal carbonisation of pretreated PEFB]
	- Chemical activation of hydrochars from hydrothermal carbonisation
	- Chemical activation of pretreated PEFB hydrochars

Note: *Palm empty fruit bunch

Up to 10 types of Thai agricultural residues will be employed to study the effect of operating conditions and different constituents of biomass on carbon yields and properties. Activated carbons, lignin and cellulose commercially available will also be investigated for comparison.

MTEC/NSTDA (Sumitra's research group) who has gained expertise in thermochemical conversion of biomass and Kyoto University (Abe's research group) who has accumulated knowledge on energy storage devices, e.g. lithium-ion batteries and supercapacitors, have a mutual interest in developing activated carbons for this particular use. This joint collaboration will, thus, provide a technology platform of carbon materials for energy storage applications from upstream raw materials to end-use products. This work will be jointly collaborated between MTEC/NSTDA, responsible for producing carbon from biomass and performing physical characterisation of the obtained carbon, and Kyoto University, in charge of conducting electrochemical characterisation of the carbons.

2.2 Literature Review

2.2.1 Lithium-ion battery

Currently, lithium-ion battery (LIB) has been widely used as not only a power source for portable electronic devices but also batteries for applications which require higher power and energy densities as well as longer cycling life such as electric vehicles or hybrid electric vehicles. This is due to the fact that LIB provides advantages of high voltage, high energy density, long cycling life, good environment compatibility and light weight over conventional batteries.

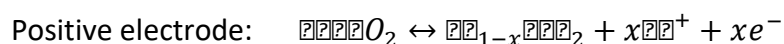
2.2.1.1 Principle of lithium-ion battery

Four important components are present in all of the lithium-ion batteries.

- Cathode or positive electrode. The positive electrode materials are typically divided into: 1) Li-containing metal oxides with a layered structure (such as LiTiS_2 , LiCoO_2 , $\text{LiNi}_{1-\gamma}\text{Co}_\gamma\text{O}_2$); 2) tunnel-structured materials (such as lithium manganese oxide).
- Anode or negative electrode. The negative electrode materials can be categorised into: 1) insertion-type materials (such as carbon, $\text{Li}_4\text{Ti}_5\text{O}_{12}$, TiO_2); 2) conversion-type materials (iron oxides, nickel oxides, cobalt oxides, etc.); 3) alloying-type materials (such as Si, Sn, etc.). Commercial anode LIBs are usually made from carbonaceous anode materials in which Li is inserted or intercalated during charging.
- Electrolyte. The electrolyte functions as a transporting medium of the positive lithium ions between the positive and negative electrodes. Lithium salt, such as LiPF_6 , is the most commonly used electrolyte.
- Separator. The separator is used to isolate the positive and negative electrodes. It is an important element to prevent short circuiting between the two electrodes. Polyolefins, such as polyethylene polypropylene, are used as a separator in the commercially available lithium-ion cells.

Figure 2-1 shows how the lithium-ion batteries work. Basically, when the battery is charging up or, in the other words, the battery takes in and stores energy, the positive electrode, i.e. lithium-cobalt oxide, gives away some lithium ions which then moves to the negative electrode, i.e. graphite, through electrolyte. These lithium ions are stored between layers of graphene in the graphite electrode. When the battery is discharging, the lithium ions move back across the electrolyte to the positive electrode. Again, the lithium ions sit in layers between layers of cobalt ions and oxide ions. In summary, when the battery charges and discharges, lithium ions move back and forth from one electrode to the other.

The electrochemical reactions inside the lithium-ion cell can be described as follows:



Negative electrode: $\text{Me}_6 + x\text{Li}^+ + xe^- \leftrightarrow \text{Me}_x\text{Me}_6$

Total cell reaction: $\text{Me}_2\text{O}_2 + \text{Me}_6 \leftrightarrow \text{Me}_{1-x}\text{Me}_2 + \text{Me}_x\text{Me}_6$

where 1) Me = Metal.

2) The forward reaction is charging while the backward reaction is discharging.

Lithium-ion battery is composed of the following four elements:

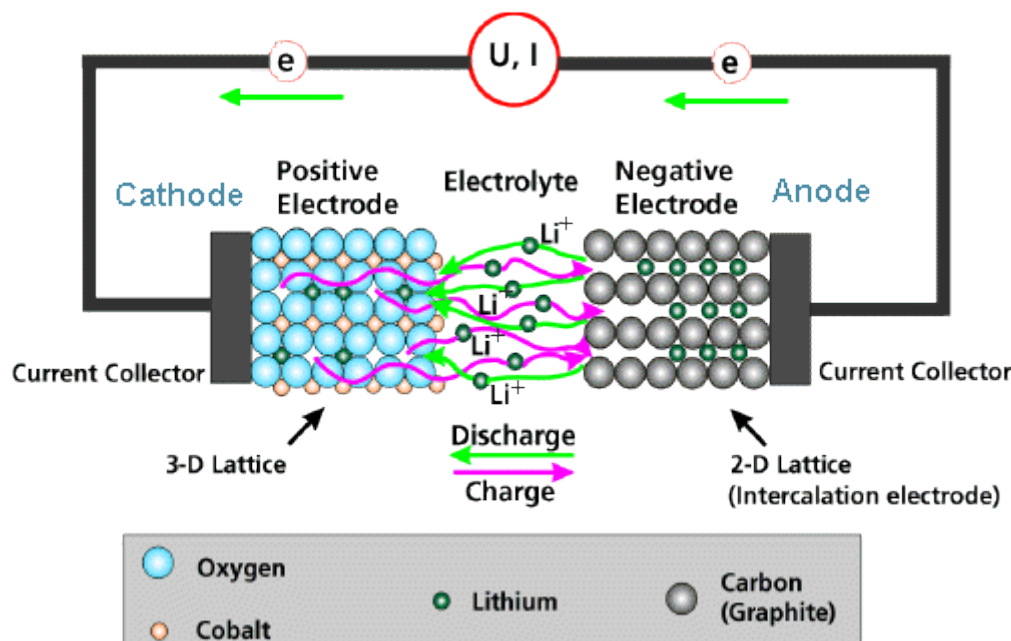


Figure 2-2 Principle of lithium-ion battery [1]

2.2.1.2 Carbon as components in positive electrodes

Carbon can be used in positive electrodes as conductive additives in positive electrodes as described below.

Conductive additives

Conductive additives in positive electrodes are necessary to provide sufficient electronic and thermal conductivities. Since the conductive carbons only enhance the electrical resistivity but are not involved in the electrochemical reactions, or in the other words, the amount of the conductive carbon must be minimised.

✓ Graphite conductive additives

The type of graphitic powder generally used as conductive additive is highly crystalline graphite material. Graphite conductive additives can be produced from either natural source or manufacturing synthesis. For synthetic graphite powders, the amorphous high-purity carbon precursors, like petroleum cokes and coals, are graphitised above 2,500°C under oxygen-free environment to form crystalline carbon. Typically, an average particle size below 10 μm for graphite conductive additives is required in the positive electrode. In addition to the particle size distribution, the graphite morphology plays a significant role in the conductivity of the electrode

mass, e.g. particles with the anisometric morphology exhibit a higher conductivity in the positive electrode than those with the isometric morphology.

✓ Conductive carbon blacks

Conductive carbon blacks are known as highly structured aggregates of primary carbon particles which have a concentric morphology composed of repeating carbon layers. Acetylene black produced by the thermal decomposition of acetylene at above 800°C is one of the conventional and well-known conductive carbons. Highly structured carbon black, which is of high void volume, is desirable since less concentration of carbon black in the positive electrode is required.

✓ Fibrous graphite materials

Due to its low bulk densities, the vapour-grown carbon fibre is produced by exposing a metallic catalyst to a mixture of hydrocarbon gases and hydrogen at above 1,000°C. In addition, its high intrinsic electronic and thermal conductivities lend itself as a conductive additive in battery electrodes.

2.2.1.3 Carbon as components in negative electrode

Negative electrode

✓ Hard carbons

Hard carbon is mechanically hard and are not graphitisable by heat treatment. This type of carbon is mostly obtained from the carbonisation of thermosetting polymers, cellulose, charcoal, coconut shells, etc. The reason that the graphitic structure from hard carbon cannot be formed by heat is there are strong sp^3 crosslinking bonds which obstruct the rearrangement of the carbon atoms to form the layer structure of graphite. Hard carbon is suitable for power-oriented lithium-ion batteries, i.e. requiring low energy densities but short charging or discharging. Commercial hard carbons are produced by pyrolysis of petroleum pitch, cross-linked phenolic resins or polymers (PVC, PAN or PFA).

✓ Graphitised mesocarbons

Mesophase carbon is an optically anisotropic liquid crystalline phase formed by heat treatment of organic pitch components between 400°C and 500°C. The steps of mesophase development are as follows: 1) Thermal decomposition of the precursor to form polycondensed aromatic molecules; 2) the growth of these molecules into layers; 3) the development of spheres which grow into layers and a continuous mesophase is produced. These spheres, called mesocarbon microbeads or MCMB, exhibit interesting properties for lithium-ion batteries. MCMB is considered as a benchmark for lithium-ion batteries as they are the mostly used carbonaceous negative electrode materials in the batteries. The characteristics of MCMB are low BET specific surface area and isotropically oriented crystalline domain.

✓ Coated natural graphites

Natural graphite is an attractive material for negative electrode as it has features which are needed to improve the energy density of portable lithium-ion batteries. However, the disadvantages of natural graphite in negative electrode is high BET specific surface area as well

as the softness and the anisometry of the particles. Thus, to minimize these drawbacks, natural graphite electrode materials are spherically fabricated and coated with hard carbon.

✓ **Synthetic graphites**

The synthetic graphites are typically isotropic soft carbon with high graphitisation degree. The required properties are low BET specific surface area, high crystallinity and high real density. Synthetic graphite is generally produced by heat treatment of a precursor carbon such as petroleum coke at high temperatures (2,800°C or higher).

✓ **Carbon-based hybrid materials**

In order to extend the performance of the negative electrode in lithium-ion batteries, carbon-based hybrid materials have been considered. A finely nano-sized metal or alloy partially replaces the carbon to produce the carbon-based hybrid materials. The examples are a silver coating of graphite, a dispersion of nano-sized silicon in the carbon, etc.

Conductive additives

It seems that the conductive additives are not essential in the negative electrodes; however, they are generally employed in the commercial electrodes to control the electronic and thermal conductivity. Carbon black, graphite and carbon fibre as mentioned in Section 2.1.2.1 are usually used in combination with commercial electrode materials. The quantity of the additives is preferably small (below 1%-2%) as their high BET specific surface area affects the specific charge losses of the negative electrode.

2.2.2 Supercapacitor

Supercapacitors have been developed for applications which required energy pulses during short periods. They provide a higher energy density than dielectric capacitors and a higher power density than batteries.

2.2.2.1 Principle of supercapacitor

Supercapacitor is, fundamentally, composed of two identical electrodes immersed in an aqueous or organic electrolyte. The two electrodes are separated by a separator which is a porous membrane. An electrode material is generally a nanoporous activated carbon which is coated on a current collector made from aluminium (in organic electrolyte) or stainless steel (in aqueous KOH). A binder, i.e. polytetrafluoroethylene (PTFE), carboxymethylcellulose (CMC), is employed to provide cohesion for the active carbon powder without blocking active surface area and also to enable the adhesion of the active material to the current collector. When the supercapacitor is charged, the negative ions and vacancies on the positive electrode side as well as the positive ions and the electrons on the negative electrode side are arranged across the interface. This ion arrangement, thus, gives another name 'electrical double layer capacitor (EDLC)'. As the layer of ions is formed by the physical movement of ions, unlike batteries, there is no chemical reaction involved.

2.2.2.2 Carbon as components in electrodes

✓ Activated carbon

Activated carbon is employed as both positive and negative electrodes owing to its low cost, good electrical conductivity and high specific surface area. Activated carbon can be produced from carbonaceous precursors, e.g. coal, wood, etc., by either physical or chemical activation or a combination of both. While physical activation is the heat treatment of carbon precursor at relatively high temperatures (up to 1,200 °C) in the presence of steam or CO₂ or air, chemical activation is, in general, conducted at lower temperatures (from 400°C to 700°C) with the presence of porogen such as phosphoric acid, potassium hydroxide, sodium hydroxide and zinc chloride.

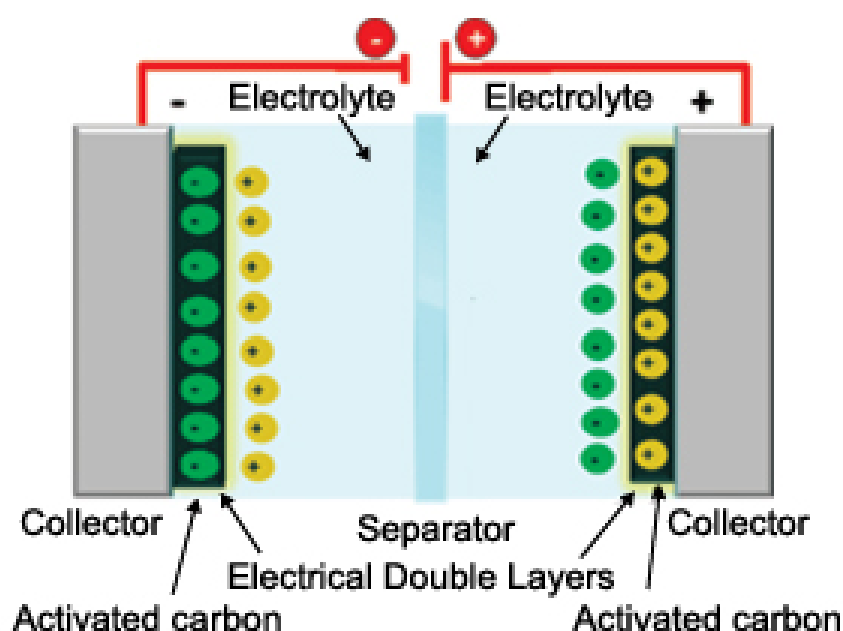


Figure 2-3 Principle of supercapacitor [2]

✓ Templated carbons

Templated carbon is considered as a good material for electrodes as it offers well-controlled pore size, large specific surface area and interconnected pore network. The template method includes: 1) infiltration of carbon precursor into the pores of the template; 2) polymerization or carbonisation; 3) removal of template to obtain templated porous structure.

✓ Carbon nanotubes (CNT)

Carbon nanotubes offer unique physical properties, i.e. high electrical conductivity as well as good chemical and mechanical stability. There are two types of carbon nanotubes: single-walled carbon nanotubes (SWCNTs) and multi-walled carbon nanotubes (MWCNTs). SWCNTs is composed of a

cylindrical tube made of graphene sheet while MWCNTs comprise of an array of SWCNTs as shown in Figure 2-3.

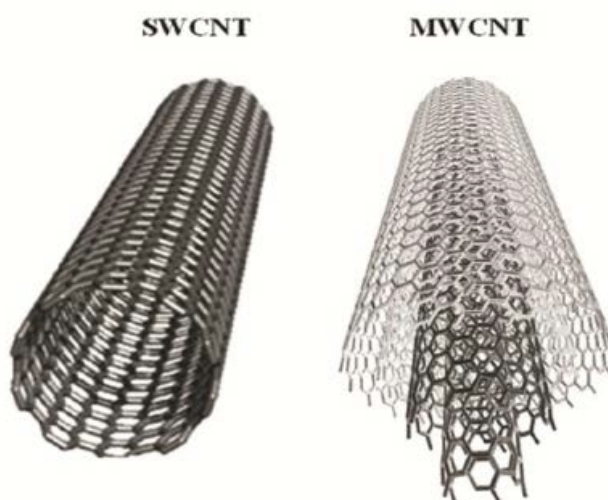


Figure 2-4 Schematics of SWCNT and MWCNT

Carbon nanotubes can be synthesised by: 1) arc discharge; 2) laser ablation; 3) chemical vapour deposition. The simplest and most popular method to produce carbon nanotube is chemical vapour deposition which is to vaporise light hydrocarbons at high temperature in the presence of nanoscale metal catalyst facilitating the growth of the carbon nanotubes.

✓ Graphene-based materials

Graphene is a single layer of graphite which, thus, offers good electronic transport properties, excellent thermal conductivity, high mechanical strength and large surface area. Many methods have been proposed to produce graphene materials, i.e. mechanical cleavage of graphite, unzipping carbon nanotubes, chemical exfoliation of graphite, solvothermal synthesis, epitaxial growth on SiC surface and metal surface, chemical vapour deposition, and bottom-up organic synthesis.

2.2.3 Research on carbon production from biomass for energy storage application

Recently, with the advancement in electric vehicles and devices, technologies for energy supplies are inevitably necessary. Li-ion battery and supercapacitors are considered as potential and promising solutions since they can effectively store energy from sustainable sources and release energy as required. The performance of energy storage devices significantly depends on the materials used as components. In the past, materials derived from unrenovable sources, .e.g rare metallic compounds, expensive polymer, etc. In order to move forward to the sustainable way of power production, it is necessary to decrease the use of non-sustainable elements in energy storage devices as well as, at the same time, increase the reliance on the renewable source. Biomass is an organic material which is a renewable and inexpensive source. Typically, as a renewable energy source, biomass can be transformed into power and energy directly through

thermochemical reactions or converted into liquid form as fuels. On the other hand, due to the demand of renewable source of elements in energy storage devices, carbon-based materials from biomass can replace those from the non-renewable sources. Research on carbon production from biomass for energy storage application has been recently focused. Previous works on supercapacitors and Li-ion batteries published in chronological order are shown in Table 2-1 and Table 2-2, respectively.

Table 2-2 Research on carbon materials for supercacacitor (arranged in chronological order)

Precursor	Carbon material product	Production method
Banana fibre [3]	Activated carbon	- Chemical activation (KOH and ZnCl ₂ – wet mixing) at 800°C
Cherry stones [4]	Activated carbon	- Immersion with H ₂ SO ₄ - Chemical activation (H ₃ PO ₄ , ZnCl ₂ , KOH – wet mixing) at 400-900°C under N ₂
Coffee endocarp [5]	Bindless monolithic electrode	Carbonisation at 600°C under N ₂ / Physical activation with CO ₂ at 800°C / Chemical activation (KOH – wet mixing) at 650°C
Sunflower seed shell [6]	Nanoporous carbon electrode	- Chemical activation (KOH – wet mixing) at 600-800°C ----- - Pyrolysis at 400 °C under N ₂ - Chemical activation (KOH – dry mixing) at 600 °C under N ₂
Celtuce leave [7]	Porous carbon	- Pyrolysis at 600°C under Ar - Chemical activation (KOH – wet mixing) at 800 °C
Kraft cellulose, hydrolysis lignin, chips and bark from birch wood [8]	Nanoporous carbon	- (Immersion with H ₃ PO ₄) - Pyrolysis at 375-550°C under N ₂ - Chemical activation (NaOH – wet mixing) at 575-800°C Note - DOE was employed to design the matrices of experiment - Correlation model was established

Precursor	Carbon material product	Production method
Cattail [9]	Porous carbon foam	<ul style="list-style-type: none"> - (Pyrolysis at 850 °C under N₂) - Chemical activation (KOH – dry mixing) at 850 °C under N₂
Corn stalk [10]	Graphitic carbon nanosheets	<ul style="list-style-type: none"> - Immersion with K₄[Fe(CN)₆] solution - Pyrolysis at 1,100°C under Ar
Distillers dried grains with solubles (DDGS) [11]	Layered nanostructure similar to that of activated graphene	<ul style="list-style-type: none"> - Pyrolysis - Chemical activation (KOH – wet mixing) at 950 °C under N₂ - Hydrothermal oxidation with HNO₃ aqueous solution at 150°C
Hemp bast fibre [12]	Carbon nanosheet	<ul style="list-style-type: none"> - Hydrothermal carbonisation with H₂SO₄ at 180°C - Chemical activation (KOH – dry mixing) at 700-800 °C
Palm empty fruit bunch [13]	Activated carbon	<ul style="list-style-type: none"> - Pyrolysis (280°C) - Chemical activation - KOH (wet mixing) at 800°C under N₂ - Physical activation – CO₂
Paulownia sawdust [14]	Microtube bundle carbon (MTBC)	<ul style="list-style-type: none"> - Pyrolysis at 700°C under N₂ - Chemical activation (NaOH – dry mixing) at 800 °C - Fabrication into MTBC
Red cedar wood [15]	Carbon electrode	<ul style="list-style-type: none"> - Pyrolysis at 750°C under N₂ - Immersion in HNO₃ solution
Watermelon [16]	Carbonaceous hydrogel and aerogel	<ul style="list-style-type: none"> - Hydrothermal carbonisation at 180°C (hydrogel) - Freeze-drying (aerogel) - Immersion in the mixture of FeCl₃ and FeSO₄.7H₂O at 80°C (magnetite carbon aerogel)
Waste tea leaves [17]	Activated carbon	<ul style="list-style-type: none"> - Pyrolysis at 600°C under Ar - Chemical activation (KOH – wet mixing) at 800 °C
Corn stover [18]	Activated carbon	<ul style="list-style-type: none"> - Microwave pyrolysis/slow pyrolysis at 600°C)

Precursor	Carbon material product	Production method
		- Chemical activation (KOH, NaOH – wet mixing) at 820°C
Rice bran [19]	Carbon	- Pyrolysis at 700°C under N ₂ - Chemical activation (KOH) under N ₂
Sawdust [20]	Magnetic nanofiber/mesoporous carbon composites	- Immersion with FeCl ₃ , Fe ₂ (SO ₄) ₃ , Fe(NO ₃) ₃ , CuCl ₂ , NiCl ₂ - Fast pyrolysis at 600-800°C under N ₂
Sugarcane bagasse [21]	Carbon	- Hydrothermal carbonisation with H ₂ SO ₄ at 180°C - Chemical activation (KOH – dry mixing) at 700-900 °C under Ar (Chemical activation/Hydrothermal carbonisation and pyrolysis/ hydrothermal carbonisation and chemical activation)
Sugarcane bagasse and rice straw [22]	Porous carbon	- Pyrolysis at 400°C - Chemical activation (H ₃ PO ₄ – wet mixing) at 600-800°C
Watermelon [23]	Carbonaceous aerogel	- Hydrothermal carbonisation at 180°C - Hydrothermal carbonisation at 120°C with 1) KMnO ₄ and Na ₂ S ₂ O ₃ .5H ₂ O; 2) MnSO ₄ .H ₂ O and (NH ₄) ₂ S ₂ O ₈ - Pyrolysis at 350°C under N ₂
Corn cob [24]	Activated carbon	- Pyrolysis at 400°C under N ₂ - Chemical activation (KOH – wet mixing) at 800-900°C under N ₂
Fungus (Auricularia) [25]	Carbon	- Hydrothermal carbonisation with KOH at 120°C - Pyrolysis at 800°C under N ₂ ----- - Hydrothermal carbonisation at 120°C - Chemical activation (KOH – dry mixing) at 800°C

Precursor	Carbon material product	Production method
Shiitake mushroom [26]	Hierarchically porous carbon	<ul style="list-style-type: none"> - Chemical activation (H_3PO_4 – wet mixing) at $500^\circ C$ under N_2 - Chemical activation (KOH – wet mixing) at $800^\circ C$ under N_2
Waste coffee grounds [27]	Hierarchically porous carbon nanosheet (HP-CNS) and microporous carbon nanosheet (MP-CNS)	<p><u>HP-CNS</u></p> <ul style="list-style-type: none"> - Chemical activation (KOH – dry mixing) at $1,200^\circ C$ <p><u>MP-CNS</u></p> <ul style="list-style-type: none"> - Chemical activation (KOH – dry mixing) at $800^\circ C$
Yellow pine biochar [28]	Carbon	<ul style="list-style-type: none"> - Oxygen plasma ----- - Chemical activation (NaOH – wet mixing) at $950^\circ C$ under N_2
Natural cotton [29]	Carbon fibre aerogel	<ul style="list-style-type: none"> - Pyrolysis at $800^\circ C$ under N_2 - Chemical activation (KOH – wet mixing)
Sugarcane bagasse [30]	Nitrogen-rich porous carbon	<ul style="list-style-type: none"> - Immersion with $CaCl_2$ / KOH / $ZnCl_2$ in the presence of urea - Pyrolysis at $800^\circ C$

Table 2-3 Research on carbon materials for Li-ion batteries (arranged in chronological order)

Precursor	Carbon material product	Production method
Rice husk [31]	Hard carbon	<ul style="list-style-type: none"> - (Leaching with NaOH) - (Immerse in pore-genic agent) - Leaching with HCl - Pyrolysis at $500-900^\circ C$ under Ar
Banana fibre [32]	Disordered carbon	<ul style="list-style-type: none"> - Chemical activation ($ZnCl_2$/KOH) at $800^\circ C$ under N_2
Coffee shell [33]	Carbon	<ul style="list-style-type: none"> - Chemical activation ($ZnCl_2$/KOH – wet mixing) at $800-900^\circ C$ under N_2
Coconut shell [34]	Carbon	<ul style="list-style-type: none"> - Chemical activation (KOH/$ZnCl_2$ – dry mixing) at $800-900^\circ C$ under N_2

Precursor	Carbon material product	Production method
Cornstalk [35]	Hierarchical porous carbon	<ul style="list-style-type: none"> - Pyrolysis at 400°C under N₂ - Chemical activation (KOH – wet mixing) at 800°C under N₂
Cherry stones [36]	Activated carbon	<ul style="list-style-type: none"> - Immersion in H₂SO₄ to remove inorganic components - Chemical activation (KOH/ZnCl₂ – wet mixing) at 500-800°C under N₂ <p>Note: Compare with MWCNT</p>
Olive stones and cherry stones [37]	Disordered microporous carbon	<p>Olive stones</p> <ul style="list-style-type: none"> - Pyrolysis at 700°C - Physical activation (steam) <p>Cherry stones</p> <ul style="list-style-type: none"> - Immersion in H₂SO₄ - Chemical activation (ZnCl₂ – wet mixing) at 500°C under N₂
Rice husk [38]	Carbon	<ul style="list-style-type: none"> - Chemical activation (proprietary porogenic agent – wet mixing) at 500-900°C
Pomelo peels [39]	Carbon	<ul style="list-style-type: none"> - Pyrolysis at 900°C under Ar
Green tea leaves [40]	Carbon	<ul style="list-style-type: none"> - Pyrolysis at 700-900°C under N₂
Rice husk [41]	Activated carbon	<ul style="list-style-type: none"> - Immersion in HCl to remove metallic oxides - Pyrolysis at 550°C under Ar - Chemical activation (KOH – dry mixing) at 800°C under Ar
Natural silk [42]	Hierarchical porous nitrogen-doped carbon (HPNC) nanosheets (NS)	<ul style="list-style-type: none"> - Chemical activation (ZnCl₂ in FeCl₃ solution – wet mixing) at 900°C under N₂
Peanut shell [43]	Hard carbon	<ul style="list-style-type: none"> - Pyrolysis at 500-1,000°C - ----- - Chemical activation (KOH – wet mixing) at 600°C - Immersion in ZnCl₂/K₂CO₃/H₃PO₄

2.2.4 Summary of literature review and scope of the present study

According to Table 2-1 and Table 2-2, there are a number of carbon material products from biomass which have been attempted to synthesise recently. Of all, activated carbon is the product which has been extensively focused. This is likely due to its broad use as elements in energy storage devices. This work will also highlight on the production of activated carbon (AC).

While previous efforts have been made to produce activated carbons from myriad types of biomass, it is not possible to compare among data from different works. It is due to the fact that many parameters play important roles in carbonisation and activation for the production of activated carbons and, also, they rely specifically on experiment design/configuration. Even though some few remarks can be inferred from different works which studied the same precursor biomass, conclusive results based on the biomass constituents cannot be made because of the discrepancies among experimental setups. One of the objectives of this work, thus, aims to gain better understanding of the impact of precursor constituents on the electrochemical properties as elements in energy storage devices. This scope also extends to explore the usage possibility of agricultural residues in Thailand as raw materials for energy storage devices with different pyrolysis methods, i.e. carbonisation and hydrothermal carbonisation, as well as different porogens in chemical activation step.

In addition, the production of activated carbons from the 'trivial' biomass, i.e. biomass mainly containing carbon, has been widely explored while the 'challenging' biomass, i.e. biomass containing significant amount of ash, has not been established yet. This, hence, will set as the second main aim of the work.

2.3 Experimental

2.3.1 Biomass samples

Up to 10 types of Thai agricultural residues will be employed to study the effect of operating conditions and different constituents of biomass on carbon yields and properties. The selected biomasses are: palm empty fruit bunch (PEFB), coconut shell, rubber wood, palm shell, corn husk, sugarcane bagasse, eucalyptus wood, eucalyptus bark, cashew nut shell and *Jatropha*. Of all, PEFB will be explored extensively. They will be acquired from either local markets or plantations. Commercially available activated carbons, lignin and cellulose will also be investigated for comparison. All types of biomass were milled by a shredder and then ground to a powder form by either a disc grinder or a rotor mill. Afterwards, the ground samples were sieved to the size of less than 75 μm ($< 75 \mu\text{m}$) and more than 150 μm ($> 150 \mu\text{m}$) and dried in an oven at 107°C for 16 hours prior to storage and use.

2.3.2 Carbonisation and activation experiments

Carbonisation

Biomass samples in the size of less than 75 μm were heated by an electric tube furnace to the carbonisation temperature of 500-1,100°C at 5°C/min under the nitrogen flow at 100 ml/min. After reaching the carbonisation temperature, the samples were held at the elevated temperature for 60 mins.

Activation

Biomass samples were mixed with 2 M KOH for 24 hours. Then, the activated biomass were washed with deionized water and 1 M ZnCl_2 and dried at 107°C. Afterwards, pyrolysis was conducted at 900°C at 5°C/min under the nitrogen flow at 100 ml/min. After reaching the pyrolysis temperature, the samples were held at the elevated temperature for 60 mins.

2.3.3 Analytical techniques

Proximate analysis

A Mettler Toledo thermogravimetric analyser was used to determine moisture (M), volatile matter (VM), fixed carbon (FC) and ash (A) contents in the precursor biomasses and their carbons. Approximately 10 mg of each sample was used in each analysis. The temperature programme is adopted from ASTM D7582-10 which is as follows:

- 1) With N_2 at the rate of 20 mL/min, heat up from 30°C to 107°C at 40°C/min
- 2) Hold at 107°C for 30 minutes
- 3) Heat up to 950°C at 30°C/min
- 4) Hold at 950°C for 7 minutes
- 5) Cool down to 600°C at 30°C/min
- 6) Hold at 600°C for 7 minutes
- 7) Switch to air flow at the rate of 8 mL/min, heat up to 750°C at 2.5°C/min
- 8) Hold at 750°C for 15 minutes

Weight loss of the sample was recorded to determine moisture, volatile matter and fixed carbon at 107°C, 950°C and 750°C, respectively, whereas ash is the residue remaining after the test.

Elemental analysis

A LECO 'CHN628' analyser is employed to determine carbon (C), hydrogen (H) and nitrogen (N) contents. Oxygen is calculated by balance according to the following equation:

$$\text{O (\%, daf)} = 100 - \text{C} - \text{H} - \text{N} - \text{Ash (\%, daf)}$$

Surface area

The surface area of carbon was characterised by N_2 adsorption at 77K using a Micromeritics '3Flex' surface characterisation analyser.

Scanning electron microscope

A Hitachi 'SU8230' FE-SEM with 5kV accelerating voltage was employed to investigate the morphology of the sample. Samples were coated with prior to observation to enhance the resolution.

Raman Spectroscopy

Raman spectra of the samples were obtained from a Bruker Optics 'Senterra' Dispersive Raman Microscope using a laser excitation wavelength of 532 nm.

2.4 Results and Discussion

2.4.1 Properties of biomass samples

Properties of biomass samples employed in this work were determined and tabulated in Table 4-1. Note that while analysis data of coconut shell is completely obtained, those of others are still pending but will be obtained soon.

Table 4-4 Property of biomass samples

Analysis	Coconut shell	PEFB	Rubber wood	Sugarcane bagasse	Palm shell
Proximate analysis					
Volatile matter (% db)	83.52	pending	pending	pending	pending
Fixed carbon (% db)	16.48	pending	Pending	pending	pending
Ash (% db)	n/d	pending	pending	pending	pending
Ultimate analysis					
C (% db)	50.71	44.53	49.65	45.17	pending
H (% db)	5.93	5.87	5.68	6.06	pending
N (% db)	0.10	1.38	6.06	0.52	pending
O (% db)	43.27	pending	pending	pending	pending
Biomass constituents					
Lignin (% db)	33.36	pending	pending	6.67	46.69
Cellulose (% db)	43.26	pending	pending	29.02	32.97
Hemicellulose (% db)	12.82	pending	pending	24.00	12.94
Others* (% db)	10.56	pending	pending	Pending	Pending

Note: *Others includes extraction, e.g. protein, fat, etc.

Ultimate analysis of the biomass samples shows that their elemental compositions do not quite differ. However, in terms of biomass constituents, sugarcane bagasse which is an

agricultural residue clearly contains different ratio of lignin, cellulose and hemicellulose from coconut shell and palm shell.

2.4.2 Characterisation of char samples

This section will present data of coconut shell and palm empty fruit bunch which are available up to now.

Proximate analysis

Proximate analysis of coconut shell (in **Table 4-1** Property of biomass sample) and its carbonised products (in Figure 4-1) clearly points out that carbonisation process removes mainly volatiles (from 83.52% to 9.33% at 1,100°C) and, thus, the fixed carbon is present in the major fraction (from 16.48% to 89.83% at 1,100°C). Also, Figure 4-1 shows that carbonisation at high temperature results in high fixed carbon and low volatiles. Regarding the proximate analysis of palm empty fruit bunch, results will be obtained soon and it is expected that the correlation between temperature and elemental composition of palm empty fruit bunch is in accordance with that of coconut shell but with a greater amount of ash content.

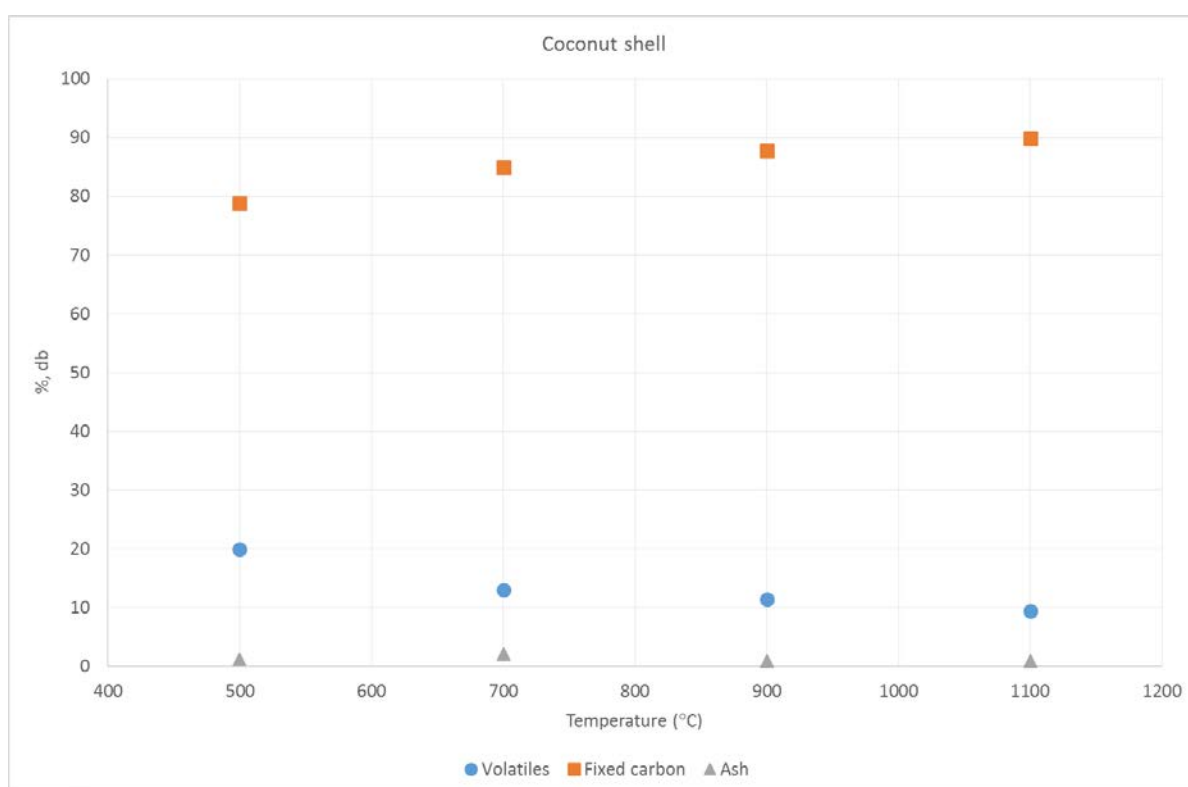


Figure 4-5 Proximate analysis of coconut shell chars carbonised at 500-1,100°C

Elemental analysis

Elemental compositions of coconut shell and PEFB are shown in Figure 4-2 and Figure 4-3, respectively. It can be seen in both types of biomass that carbon content increases after carbonisation and this is slightly intensified with increasing temperature. Also, an increase in temperature results in the reduction of oxygen and hydrogen due to the dehydration reaction. Note that PEFB contains higher ash content and this, thus, results in the lower carbon content of PEFB chars after carbonisation.

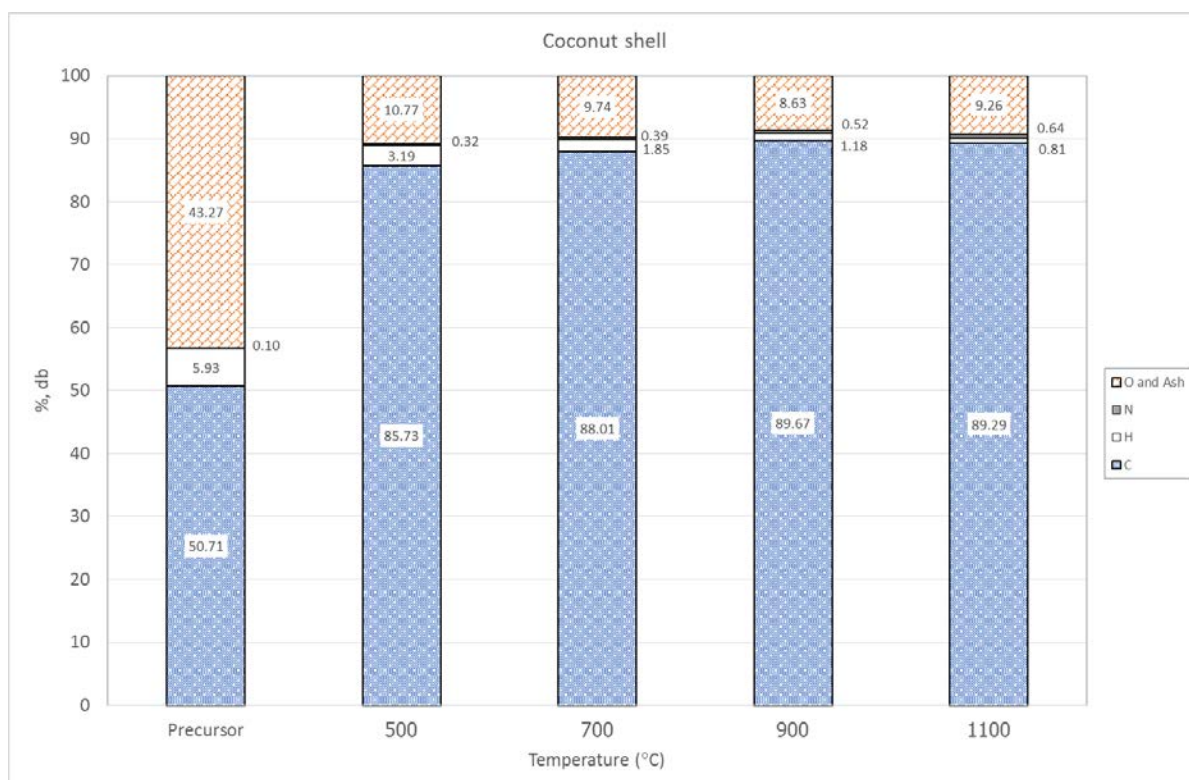


Figure 4-6 Elemental analysis of coconut shell carbonised at 500-1,100°C

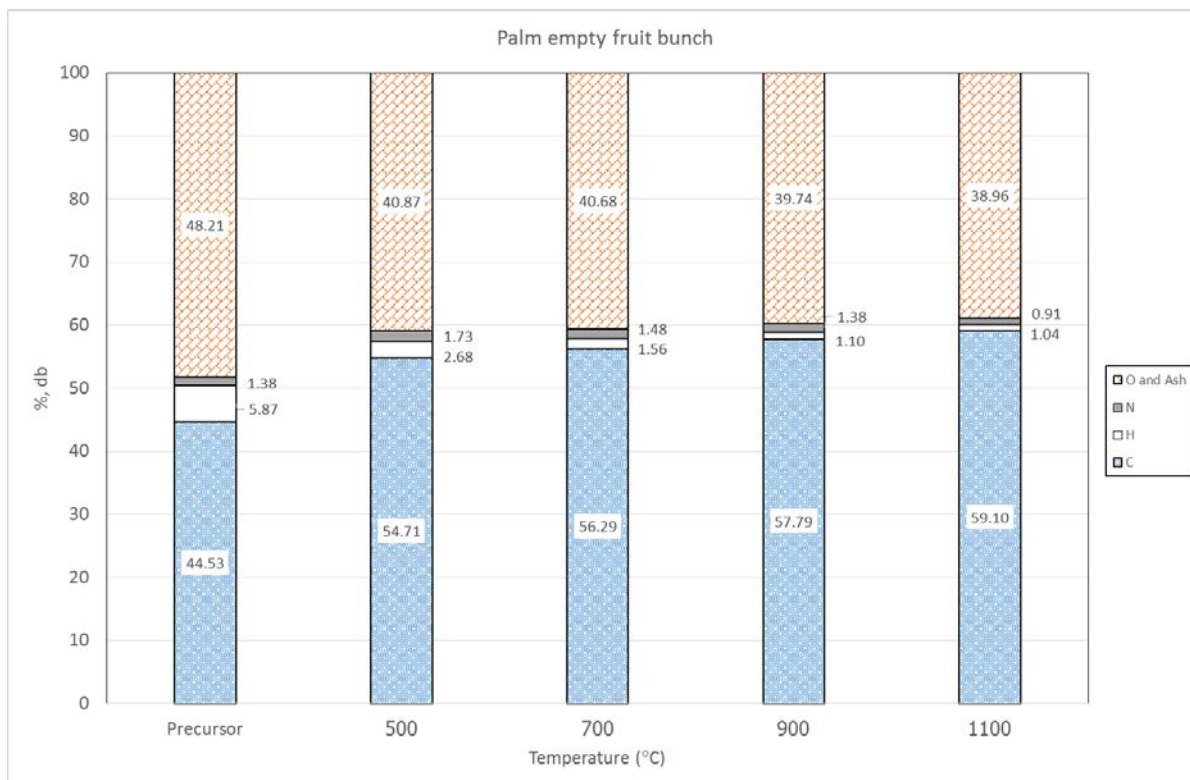


Figure 4-7 Elemental analysis of PEFB carbonised at 500-1,100°C

Surface area

BET surface area of coconut shell chars carbonised at 500-1,100°C is shown in Figure 4-4. It can be noticed that the surface area increases with temperature and levels off at 900°C.

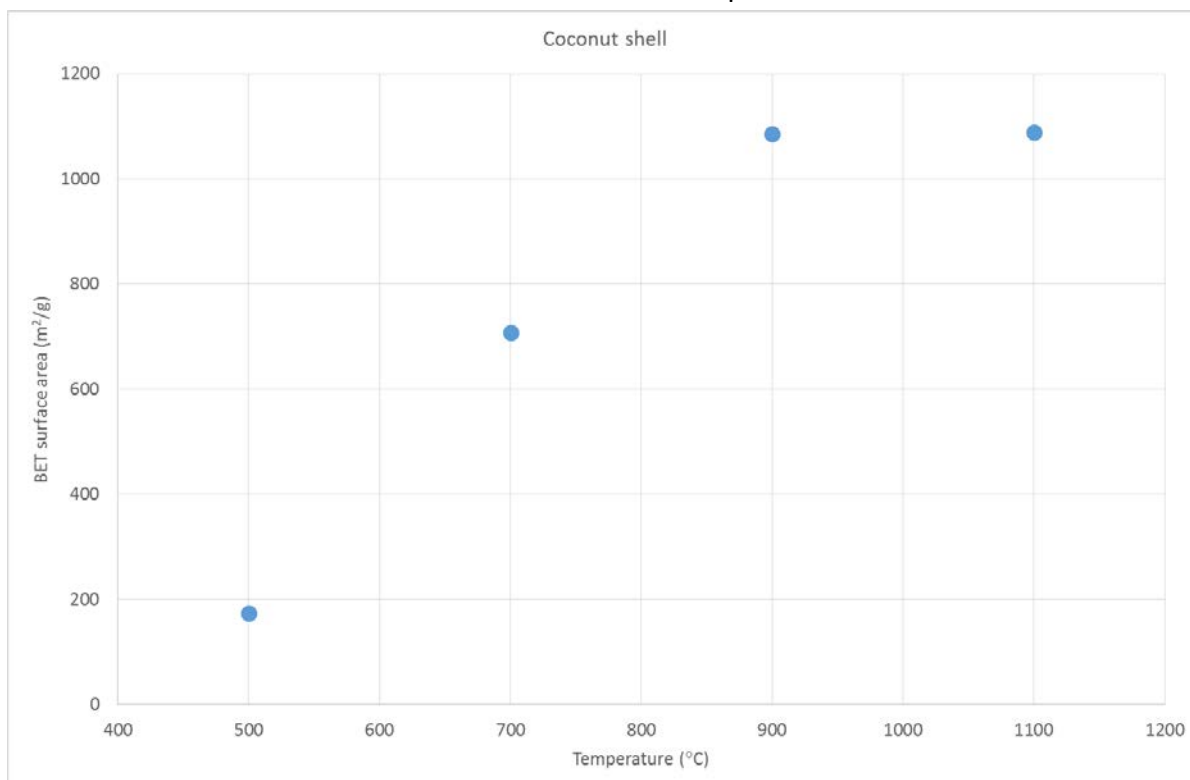


Figure 4-8 BET surface area of coconut shell chars carbonised at 500-1,100 °C

Scanning electron microscope

SEM images of coconut shell and PEFB chars carbonised at 500-1,100C are shown in Figure 4-5. It can be noticed that temperature negligibly changes morphology of chars over the temperature range of 500 to 1,100°C in both coconut shell and PEFB chars. However, dissimilarity between coconut shell and PEFB chars can be obviously seen, i.e. the surface of PEFB chars has many fine particles on.

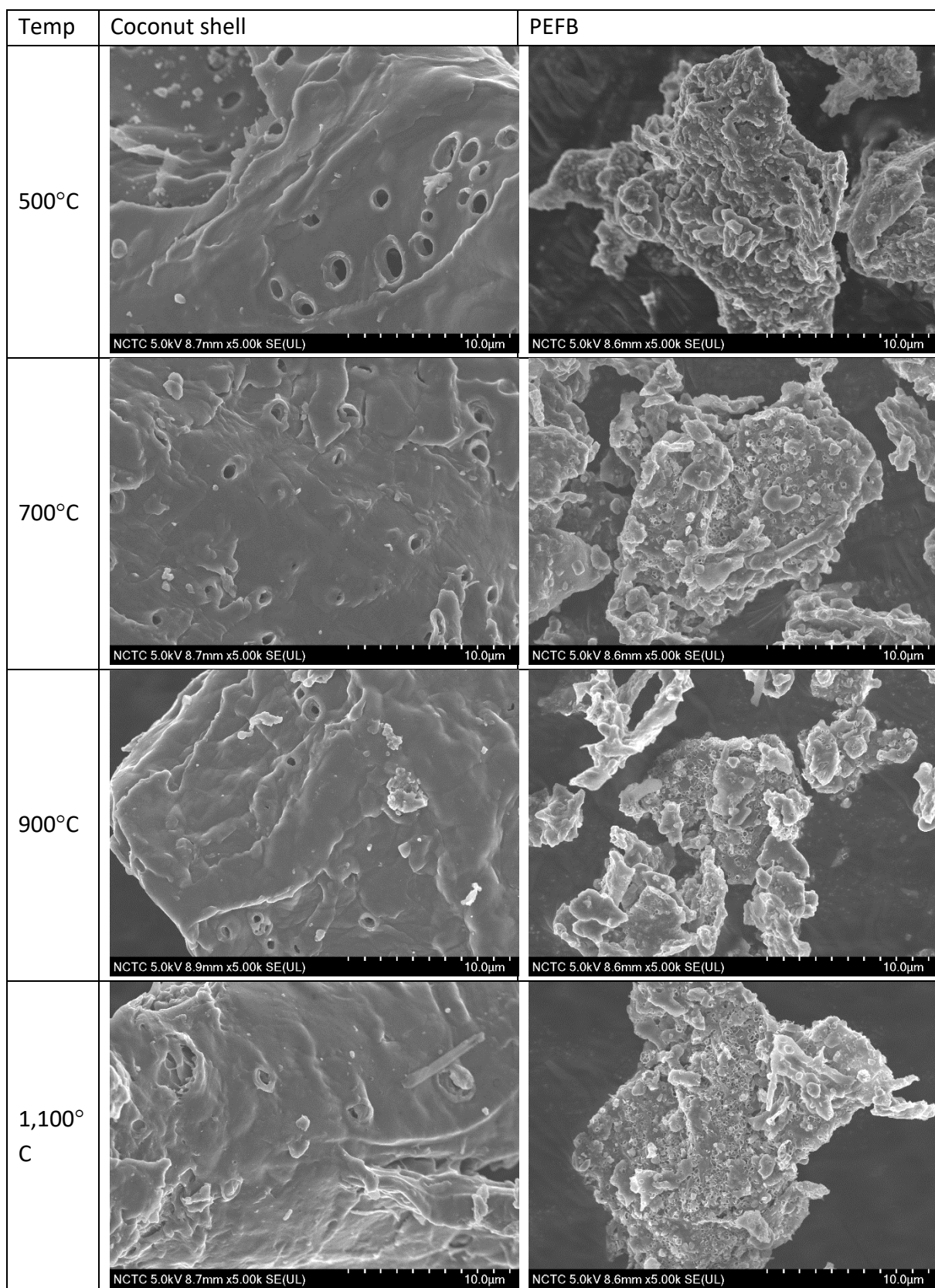


Figure 4-9 SEM images of coconut shell and PEFB chars carbonised at 500-1,100°C

Raman spectroscopy

Raman spectra of coconut shell and PEFB chars carbonised at 500-1,100°C is shown in Figure 4-6 and Figure 4-7, respectively. Spectra of both coconut shell and PEFB chars exhibit 2 peaks centered at 1,350 and 1,550 cm^{-1} . These two characteristic peaks, so-called D peak and G peak, respectively, are also present in the graphitic carbon but with spiky shape, i.e. narrow linewidth). For the present work, the linewidth of both peaks implies an amorphous carbon which exists various numbers of carbon clusters which are of different sizes and different environments. Moreover, the intensity ratio of D peak to G peak appears to increase with temperature. More data from other characterisations are needed to discuss on the ratio of D peak and G peak.

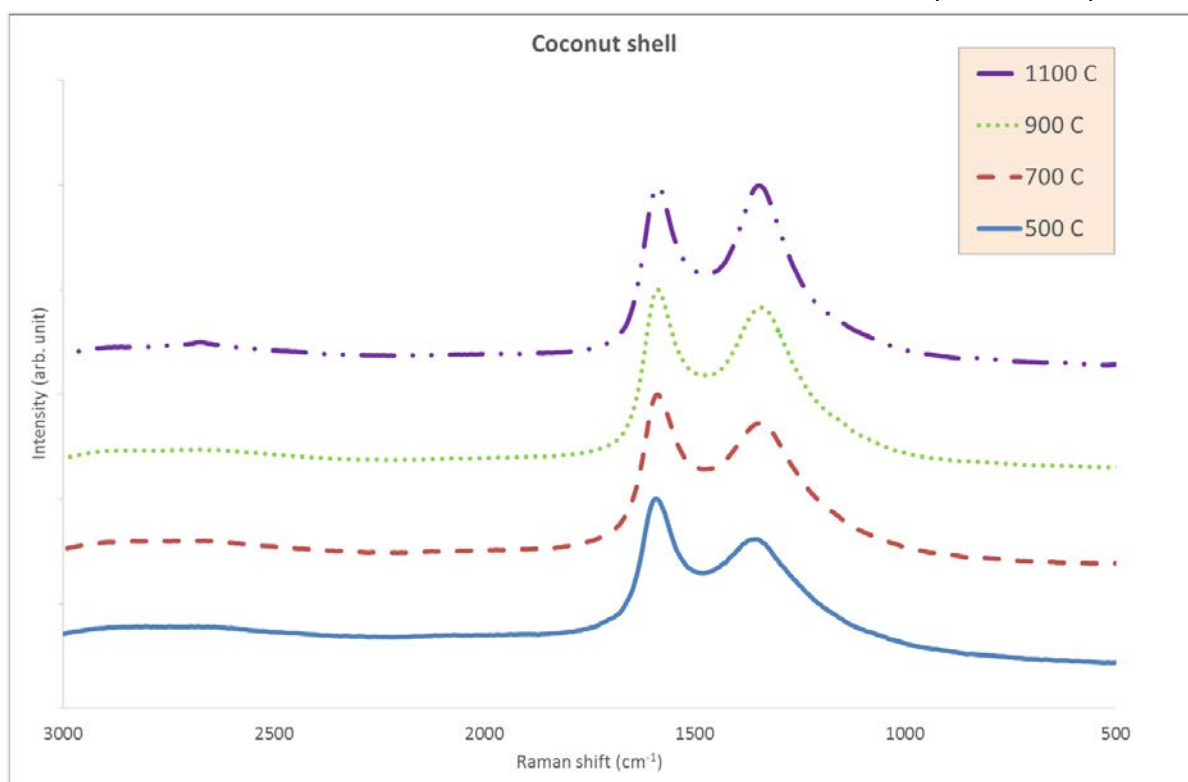


Figure 4-10 Raman spectra of coconut shell chars carbonised at 500-1,100 °C

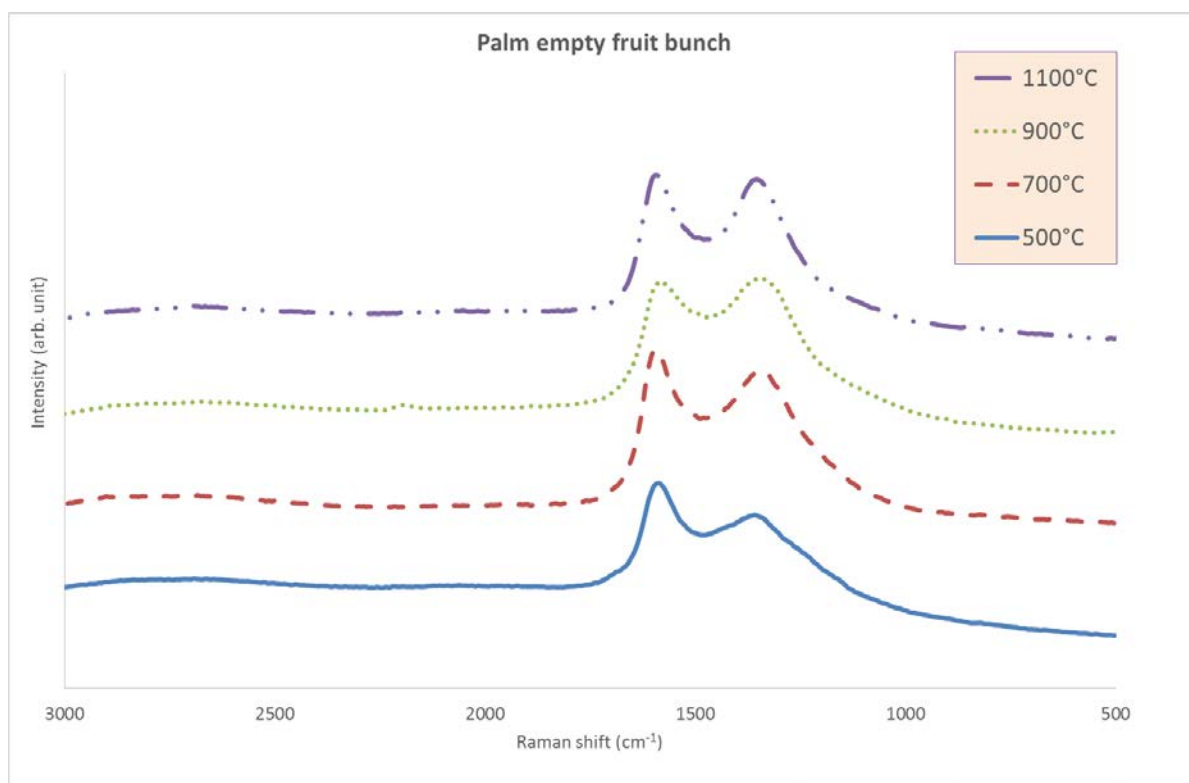


Figure 4-11 Raman spectra of PEFB chars carbonised at 500-1,100 °C

Concluding remarks

Section 2.4.2 provides the characterisation results of coconut shell and PEFB chars produced at the carbonisation temperature of 500-1,100°C. It can be noticed that high carbonisation temperatures yield chars with high carbon content, high fixed carbon content, high surface area. The carbonisation step in the activation experiment was conducted at 900°C as negligible difference of char properties, particularly surface area, between 900°C and 1,100°C could be observed.

2.4.3 Characterisation of activated carbon samples

Activation of PEFB samples in the size range of both less than 75 µm and more than 150 µm has been conducted. It was found that carbon prepared from the less-than-75-micron fraction could not be processed further: the solution of biomass and KOH appeared to be slurry and became hard after drying at 107°C. On the other hand, the activation of the more-than-150-micron fraction was successfully done. The results from the latter will, thus, be discussed below.

Elemental analysis

Elemental compositions of coconut shell and PEFB which were carbonised and activated at 900°C are tabulated in Table 4-2. For coconut shell, insignificant difference of elemental compositions between carbonisation and activation can be observed. As per PEFB, nevertheless, elemental

composition, especially carbon content, changes dramatically. This is caused by KOH solution employed in the activation process dissolves the inorganic element in the PEFB which is present in high fraction. Overall, activation process would rather impact the surface area and porosity which will be determined further.

Table 4-5 Comparison of elemental composition of coconut shell and PEFB

Biomass	Process	C	H	N	O and ash
Coconut shell	Precursor	50.71	5.93	0.10	43.27
	Carbonisation (900°C)	89.67	1.18	0.52	8.63
	Activation (900°C)	88.10	0.94	0.64	10.32
PEFB	Precursor	44.53	5.87	1.38	48.21
	Carbonisation (900°C)	57.79	1.10	1.38	39.74
	Activation (900°C)	79.36	1.25	0.86	18.54

2.5 Conclusions

Work progress on the 2016 JFY (2016.4 – 2017.3) can be summarised as follows:

1. Chars from coconut shell and PEFB were produced at different temperatures. A number of characterisation tools were employed to gain more understanding of the chars produced. It has been found that high carbonisation temperatures yield chars with high carbon content, high fixed carbon content, high surface area.
2. Activated PEFB chars could be produced by the KOH activation. The carbonisation temperature of 900°C was chosen due to the fact that properties of 900°C chars according to carbonisation experiments are comparable to those of 1,100°C chars. More characterisation techniques will further be conducted.
3. Electrochemical performance tests, of which Kyoto University is in charge, has not been performed yet. MTEC/NSTDA will collect an ample amount of samples to deliver to Kyoto University for further analyses.

2.6 Outputs

Outputs from the 2016 JFY (2016.4 – 2017.3) are listed below:

- Chars from the carbonisation of coconut shell and PEFB
- Activated carbons from the activation of PEFB

Innovations in Biomass Application for Catalytic Material Synthesis and Energy Devices

3. Innovations in Biomass Application for Catalytic Material Synthesis and Energy Devices

Research team:

Assoc.Prof.Dr. Noriaki Sano, Kyoto University (PI, Japan side)

Dr. Kajornsak Faungnawakij, NANOTEC, NSTDA (PI, Thailand side)

Dr. Vorranutth Itthibenchapong, NANOTEC, NSTDA

Dr. Pongtanawat Khemthong, NANOTEC, NSTDA

Dr. Sanchai Kuboon, NANOTEC, NSTDA

Dr. Supawadee Namuangruk, NANOTEC, NSTDA

Dr. Chompoonut Rungnim, NANOTEC, NSTDA

Dr. Pussana Hirunsit, NANOTEC, NSTDA

Dr. Chalida Klaysom, Chulalongkorn University

Assoc.Prof. Tawatchai Charinpanitkul, Chulalongkorn University

Dr. Sareeya Bureekaew, VISTEC

Miss. Chuleeporn Luadthong, NANOTEC, NSTDA

Miss. Rungnapa Kaewmeesri, NANOTEC, NSTDA

3.1 Purpose of Collaborative Research

The catalytic production of carbon-based materials, biofuels and biochemicals is a key activity in biorefinery industry. Also, developments in catalytic energy conversion and energy storage using bioactivities are important for sustainable societies. Consequently, searching for renewable resources that are reliable, sustainable and environmentally friendly is the big challenge, and these lead to green concepts including biorefinery and bio-energy devices where renewable resources drive the world. Under such circumstances, the collaborative researches carried out by the groups in NANOTEC/NSTDA (Faungnawakij's team) and Kyoto University (Sano's team) will attack this issue via accumulating innovative knowledge about biomass conversion to useful materials and development of bio-energy devices.

3.2 Research Progress

3.2.1 Development of magnetic catalysts for biodiesel production – the Fe-based catalysts have been developed for biodiesel production using palm oil and methanol as feedstocks

Copper ferrite spinel oxide (CuFe_2O_4) samples with calcination temperatures ranging from 500 to 900 °C were synthesized using the sol-gel combustion method with citric-nitrate precursors. Each calcined sample was further characterized and carefully analyzed for its structure, morphology, porosity, magnetic property and reducibility. For the first time, the catalytic

performance of the ferrite spinels was examined for palm oil methanolysis. The characterization results from X-ray diffraction (XRD), extended X-ray absorption fine structure (EXAFS) and X-ray absorption near edge structure (XANES) analyses revealed that the major part of the active species was divalent ions of Cu^{2+} and Fe^{2+} and that they played a crucial role in the activity of the considered spinel catalysts. The catalytic behaviors strongly depended on the crystallinity of spinel structures and operating parameters, such as the catalyst loading and methanol to oil molar ratio. The CuFe_2O_4 calcined at $700\text{ }^\circ\text{C}$ was the most active and selective for methanolysis with palm oil. No activity decline was observed over the catalyst after it was reused for 5 cycles without any post-treatment. Easy and effective catalyst separation could be obtained when magnetization was applied to the magnetic spinel catalysts.

Table 1. Physical and chemical properties of pristine and functionalized MWCNTs.

Catalysts	I_D/I_G ^{a)}	Cobalt concentration (wt.%) ^{b)}	The total acid site concentration ($\mu\text{mol}\cdot\text{g}^{-1}$) ^{c)}	Surface area and porosity ^{d)}		
				Pore diameter (nm)	Pore volume ($\text{cm}^3\cdot\text{g}^{-1}$)	S_{BET} ($\text{m}^2\cdot\text{g}^{-1}$)
MWCNTs	1.82	3.2	58.9 ± 42.5	3.3	0.399	135.3
p-MWCNTs	1.64	0.5	134.6 ± 42.5	3.3	0.465	132.7
c-MWCNTs	1.70	0.9	164.7 ± 50.3	3.2	0.475	133.0
n-MWCNTs	1.76	0.6	231.7 ± 39.0	3.2	0.461	130.3
s-MWCNTs	1.22	0.9	309.1 ± 34.2	3.3	0.516	131.0

^{a)} by Raman spectroscopy

^{b)} by XRF

^{c)} by titration (Boehm method)

^{d)} by N_2 adsorption-desorption isotherms measured

Table 2. Catalytic activity of D-xylose dehydration at $170\text{ }^\circ\text{C}$ for 3 h under N_2 pressure of 15 bar.

Catalysts	Xylose conversion (%)	Furfural selectivity (%)
no catalyst	34.1 ± 6.4	57.6 ± 7.1
MWCNTs	80.6 ± 1.7	43.2 ± 2.4
n-MWCNT	73.6 ± 0.2	54.0 ± 2.2
c-MWCNTs	75.8 ± 3.9	50.2 ± 6.9
p-MWCNTs	60.9 ± 3.4	49.4 ± 0.2
s-MWCNTs	62.7 ± 0.4	57.1 ± 2.0
3%Co/s-MWCNTs	95.0 ± 2.4	30.4 ± 2.7

Fig. 1 Magnetic hysteresis loop of the ferrite spinels

Fig. 2 Biodiesel (FAME) production with the ferrite spinels

3.2.2 Development of carbon-based catalysts for biomass conversion – the carbon-supported catalysts have been developed for cellulosic sugar to furans

Acid-functionalized multi-wall carbon nanotubes (MWCNTs) catalysts were prepared by a wet chemical sonication with various acid solutions, i.e., H_2SO_4 , H_3PO_4 , HNO_3 , and HCl . Sulfonic groups and carboxyl groups were detected on MWCNTs with H_2SO_4 treatment (s-MWCNTs), while only carboxyl groups were presented from other acid treatments. The catalytic dehydration of D-xylose into furfural was evaluated using a batch reactor at $170\text{ }^\circ\text{C}$ for 3 h under N_2 pressure of 15 bar. The highest furfural selectivity was achieved around 57% by s-MWCNTs catalyst, suggesting a positive role of the sulfonic functionalized groups. The effect of Co species was related to their Lewis acid property resulting in the enhancement of xylose conversion with low selectivity to furfural product.

3.2.3 Simulation study of hydrogen storage on carbon materials – various structures and orientation of H_2 molecules on carbon surfaces have been theoretically studied

The hydrogen storage reaction on metal doped carbon nanohorn (CNH) has been investigated by density functional theory (DFT) calculations. The models of carbon nanohorn with different number of pentagon (n) on the cone tips were generated and named as n -CNH where $n=1-6$. The sharp of the CNH cone tip considerably relates to the number of pentagon as shown each geometry in Fig. 3. The metals with high potential for hydrogen adsorptions such as titanium (Ti), nickel (Ni), palladium (Pd) and platinum (Pt) were placed as a single atom on the top of each CNH called as M- n CNH where M was type of metal (Ti, Ni, Pd and Pt) and n indicated sharp of CNH. After geometries optimization, we found that all the four metal strongly deposited on CNH tips with the binding energy in the range of 1.1-2.8 eV. In addition, the binding stability of the metal was related to the pi-orbital axis vector (POAV) or curvature of carbon forming bond with the metal. The higher POAV, the stronger of the metal binding stability.

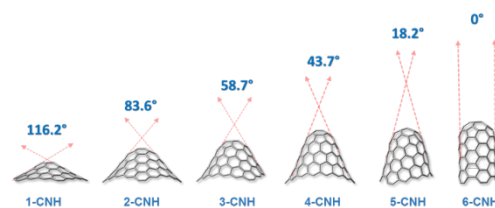


Fig. 3 Geometries of CNH with tip angle

The stability of hydrogen storage on the M- n CNH were explored by means of hydrogen adsorption energy (E_{ads}) as follow; $E_{ads} = E_{H_2/M-nCNH} - (E_{M-nCNH} + E_{H_2})$. Stronger hydrogen adsorption is implied by more negative value of E_{ads} . From the calculation result, the hydrogen adsorption relied on type of metal rather than sharp of CNH, as shown in Fig. 4. The hydrogen adsorption was in the order of Ti-CNH > Pt-CNH > Ni-CNH > Pd-CNH. The hydrogen completely dissociated when adsorbed on Ti-CNH suggested from lengthen of d(H-H) from 0.74 Å in the isolated hydrogen molecule to 2.89 Å after the adsorption. This adsorption as separated hydrogen is called dissociation mode. On the other hands, the adsorption in dissociation mode was not detected on the rest three models (Ni- n CNH, Pd- n CNH, and Pt- n CNH). The hydrogen adsorption on these M-CNHs occurred via η^2 -H₂ with weak H...H lengthening (0.8-0.9 Å) called as Kubas mode, as shown in the Fig. 5. The DFT calculation suggested that CNH doped with titanium can be applied as a potential hydrogen storage. Further details such as maximum adsorption capacity, size of metal cluster and effect of metal alloy will be next studied.

The stability of hydrogen storage on the M- n CNH were explored by means of hydrogen adsorption energy (E_{ads}) as follow; $E_{ads} = E_{H_2/M-nCNH} - (E_{M-nCNH} + E_{H_2})$. Stronger hydrogen adsorption is implied by more negative value of E_{ads} . From the calculation result, the hydrogen adsorption relied on type of metal rather than sharp of CNH, as shown in Fig. 4. The hydrogen adsorption was in the order of Ti-CNH > Pt-CNH > Ni-CNH > Pd-CNH. The hydrogen completely dissociated when adsorbed on Ti-CNH suggested from lengthen of d(H-H) from 0.74 Å in the isolated hydrogen molecule to 2.89 Å after the adsorption. This adsorption as separated hydrogen is called dissociation mode. On the other hands, the adsorption in dissociation mode was not detected on the rest three models (Ni- n CNH, Pd- n CNH, and Pt- n CNH). The hydrogen adsorption on these M-CNHs occurred via η^2 -H₂ with weak H...H lengthening (0.8-0.9 Å) called as Kubas mode, as shown in the Fig. 5. The DFT calculation suggested that CNH doped with titanium can be applied as a potential hydrogen storage. Further details such as maximum adsorption capacity, size of metal cluster and effect of metal alloy will be next studied.

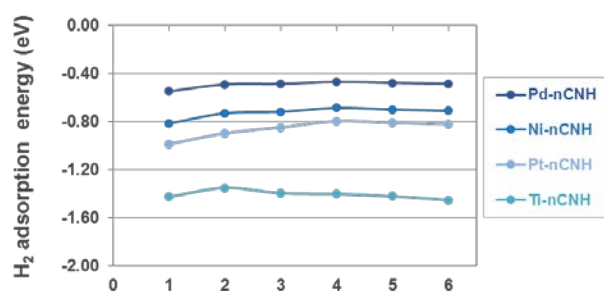


Fig. 4 Hydrogen adsorption energy on M-CNH with different sharp tips

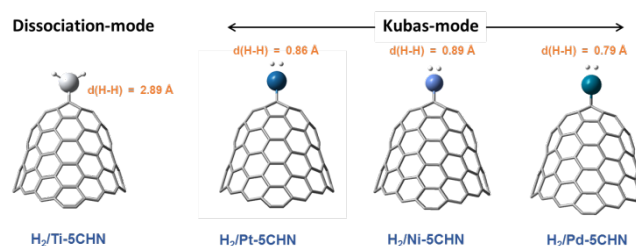


Fig. 5 Geometries of hydrogen adsorption on M-5CNH

3.2.4 Application of carbon nanotubes for microbial fuel cell—carbon nanotubes are synthesized on stainless steel electrode to enhance power generation by a microbial fuel cell

A simple microbial fuel cell (MFC) was assembled using wet soil and stainless steel plate electrodes to observe the effect of the synthesis of carbon nanotubes (CNTs) on the stainless steel

anode placed in the bottom of wet soil in glass bottle. It can be expected that the large surface area and high electrical conductivity of CNTs on the anode may enhance the power generation of the MFC. In this experiment, the soil collected from Kyoto University campus was used. Fig. 6 shows the result of I-V and V-P characteristics of the cell. It is suggested that the synthesis of CNTs can result into the increase of the power generation by more than twice.

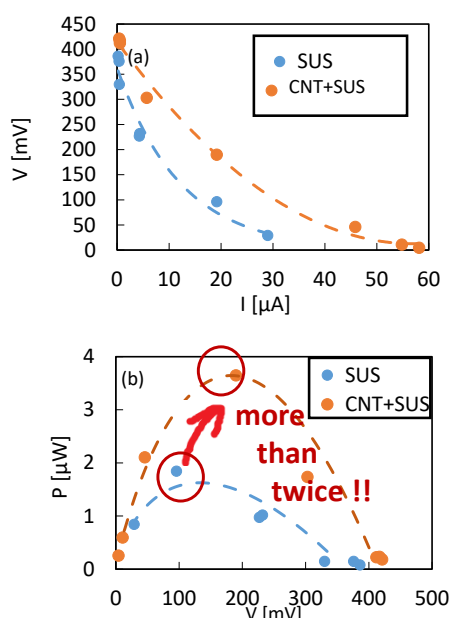


Fig. 6 (a) I-V and (b) V-P characteristics of microbial fuel cell using stainless steel (SUS) plate electrode and the one on which CNTs are synthesized.

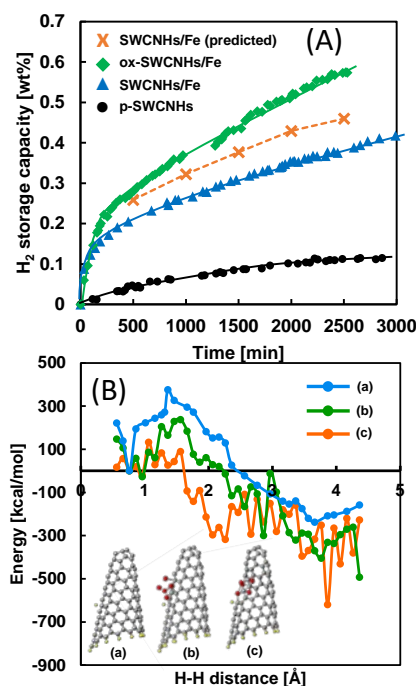


Fig. 7 (A) Results from H₂ storage measurement under 2 MPa of H₂ and 30°C. The dash line represents predicted H₂ storage capacity of SWCNHs/Fe (10 wt% of Fe) with the same Fe concentration as ox-SWCNHs/Fe (23 wt% of Fe). (B) Total energy of H₂-adsorbed structures with varied inter H-H distance.

3.2.5 Development of Fe-dispersed carbon nanohorns for H₂ storage—carbon nanohorns dispersed with Fe nanoparticles have been developed, and its H₂ storage mechanism has been investigated by molecular orbital calculation

Using gas-injected arc-in-water method developed by our group, pure-carbon single-walled carbon nanohorns (p-SWCNHs), Fe-dispersed carbon nanohorns (SWCNHs/Fe) and SWCNHs/Fe on which pores are opened by oxidation-reduction treatment (ox-SWCNHs) are synthesized. The content of Fe in SWCNHs/Fe was about 10 wt%. Fig. 7 (a) shows the H₂ uptake as function of time under a constant H₂ pressure of 2MPa. It is remarkable that only 10 wt% of Fe in SWCNHs can lead to the increase of the amount of H₂ uptake by about four times. The H₂ uptake by ox-SWCNHs/Fe is even higher than SWCNHs/Fe. In this figure, 'SWCNHs/Fe (predicted)' means the value for which Fe content in SWCNHs/Fe is same as in ox-SWCNHs. Fig. 7 (b) shows the energy change of three structures of (a) H₂-adsorbed SWCNHs, (b) H₂-adsorbed SWCNHs/Fe where Fe cluster is adsorbed on surface of SWCNHs, and (c) H₂-adsorbed SWCNHs/Fe where Fe cluster is sticking into the wall of SWCNHs, during the inter H-H distance is changed. It is suggested

that the activation energy to realize H₂ spillover effect can be significantly reduced by making Fe-sticking structure.

3.3 Outputs

3.3.1 Publication

- T. Suntornlohanakul, N. Sano, H. Tamon, Self-ordered nanotube formation from nickel oxide via submerged arc in water, *Applied Physics Express* 9, 076001 (2016)
- C. Luadthong, P. Khemthong, W. Nualpaeng, K. Faungnawakij, Copper ferrite spinel oxide catalysts for palm oil methanolysis, *Applied Catalysis A*, 525 (2016) 68-75.
- C. Termvidchakorn, V. Itthibenchapong, B. Chamnankid, S. Namuangruk, K. Faungnawakij, T. Charinpanitkul, R. Khunchit, N. Hansupaluk, N. Sano, H. Hinode, Dehydration of D-xylose to furfural using acid-functionalized MWCNTs catalysts, *Advances in Natural Sciences: Nanoscience and Nanotechnology 2017 under review*

3.3.2 Book

- Vorranutch Itthibenchapong, Atthapon Srifa, Kajornsak Faungnawakij, "Ch.11 Heterogeneous Catalysts for Advanced Biofuel Production" in "Nanotechnology for Bioenergy and Biofuel Production" Editors Mahendra Rai and Silvio Silverio da Silva, Springer 2017.

3.3.3 Award

- Presentation Award: C. Termvidchakorn, N. Viriya-empikul, K. Faungnawakij, N. Sano, T. Charinpanitkul. Catalytic activity of sulfonated carbon nanotubes in dehydration of xylose, The 4th Joint Conference on Renewable Energy and Nanotechnology (JCREN2015)
- Kajornsak Faungnawakij, TRF-OHEC-SCOPUS Researcher Award 2017

3.3.4 Student exchange

- Three students from Chulalongkorn University visited Kyoto Univ. for research exchange program under JASTIP, Oct 2016.
- Two JASTIP seminars of the project were held in 2016 at Kyoto univ. (1st, six Thai members visited Kyoto Univ.) and at NANOTEC (2nd, six Japanese members visited NANOTEC and Chulalongkorn Univ.)